NETWORKS AND HETEROGENEOUS MEDIA
©American Institute of Mathematical Sciences
Volume **4**, Number **4**, December **2009**

doi:10.3934/nhm.2009.4.755

pp. **755–788**

A MATHEMATICAL MODEL RELEVANT FOR WEAKENING OF CHALK RESERVOIRS DUE TO CHEMICAL REACTIONS

Steinar Evje* and Aksel Hiorth

International Research Institute of Stavanger (IRIS)
Prof. Olav Hanssensvei 15, NO-4068 Stavanger, Norway

Merete V. Madland and Reidar I. Korsnes

University of Stavanger (UiS)
4036 Stavanger, Norway

(Communicated by Roberto Natalini)

Abstract. In this work a mathematical model is proposed for modeling of coupled dissolution/precipitation and transport processes relevant for the study of chalk weakening effects in carbonate reservoirs. The model is composed of a number of convection-diffusion-reaction equations, representing various ions in the water phase, coupled to some stiff ordinary differential equations (ODEs) representing species in the solid phase. More precisely, the model includes the three minerals $CaCO_3$ (calcite), $CaSO_4$ (anhydrite), and $MgCO_3$ (magnesite) in the solid phase (i.e., the rock) together with a number of ions contained in the water phase and essential for describing the dissolution/precipitation processes. Modeling of kinetics is included for the dissolution/precipitation processes, whereas thermodynamical equilibrium is assumed for the aqueous chemistry. A numerical discretization of the full model is presented. An operator splitting approach is employed where the transport effects (convection and diffusion) and chemical reactions (dissolution/precipitation) are solved in separate steps. This amounts to switching between solving a system of convection-diffusion equations and a system of ODEs. Characteristic features of the model is then explored. In particular, a first evaluation of the model is included where comparison with experimental behavior is made. For that purpose we consider a simplified system where a mixture of water and $MgCl_2$ (magnesium chloride) is injected with a constant rate in a core plug that initially is filled with pure water at a temperature of $T = 130^\circ$ Celsius. The main characteristics of the resulting process, as predicted by the model, is precipitation of $MgCO_3$ and a corresponding dissolution of $CaCO_3$. The injection rate and the molecular diffusion coefficients are chosen in good agreement with the experimental setup, whereas the reaction rate constants are treated as parameters. In particular, by a suitable choice of reaction rate constants, the model produces results that agree well with experimental profiles for measured ion concentrations at the outlet. Thus, the model seems to offer a sound basis for further systematic investigations of more complicated precipitation/dissolution processes relevant for increased insight into chalk weakening effects in carbonate reservoirs.

2000 *Mathematics Subject Classification.* Primary: 76T10, 76N10, 65M12, 35L65.

Key words and phrases. water-rock interaction, physico-chemical processes, precipitation, dissolution, porous media flow, damage mechanics, convection-diffusion-reaction equations, upscaling.

The authors acknowledge BP, ConocoPhillips, and the Ekofisk Coventurers, including TOTAL, ENI, Hydro, Statoil and Petoro, for supporting the work through the research center COREC.

*Corresponding author.

1. Introduction.

1.1. Background information.

Transport and chemical reactions have been extensively studied in the recent years. The flow of aqueous reacting solutes through soil or porous rock involves a complex system of geochemical, hydrological, and biochemical processes and is of fundamental importance in many different contexts. The focus of this paper is on the study of transport and dissolution/precipitation processes relevant for weakening of chalk reservoirs.

Compaction of chalk reservoirs is experienced at the Ekofisk field in the North Sea, and is not only a result of an increase in effective stresses linked to pore pressure depletion during oil recovery. There is, however, an additional impact of the seawater injection when water replaces oil in chalks; it causes enhanced compaction of the rock, which further has shown to induce additional seabed subsidence. This phenomenon is often referred to as the *water weakening effect* on chalks.

The chemical effects of seawater like brines, Ekofisk formation water, and distilled water on the mechanical properties of high porosity outcrop chalks have been extensively studied, see [21, 32, 29] and references therein. These rock mechanical and pure core flooding studies at elevated temperatures, both on high and lower porosity chalks, have shown that the chemical composition of the saturating and flooding fluid has crucial influences on the mechanical strength of chalk. Apparently, from the studies by Heggheim et al. [21] and Korsnes et al. [29], the presence of sulphate ions SO_4^{2-} in seawater-like brines caused a significant weakening of the chalk framework, especially as the testing temperature was increased. It was suggested that chemical water weakening of chalk by seawater-like brines takes place when Mg^{2+} ions in the solution substituted Ca^{2+} ions at the intergranular contacts in the presence of SO_4^{2-} ions.

Thus, the experimental studies indicate that three ions are of particular importance, magnesium Mg^{2+}, calcium Ca^{2+}, and sulphate SO_4^{2-}, as chalk cores are exposed to seawater-like brines at increased temperatures. The published research so far, however, seems to point out that there is a rather complicated interplay between chemical reactions and transport effects. As an attempt to clarify some of these issues, recent experimental work has been carried out for some simplified water-rock systems. The objective of the work [33] was to investigate the effect of individual ions by simplifying the aqueous chemistry. In particular, some of the previously studied rock mechanical tests were repeated by using distilled water and solutions containing only $MgCl_2$.

An important part of the experimental activity is to measure ion concentrations at the outlet of core plugs and compare with the original known ion concentrations of the injected brines. Hence, a useful tool for evaluation of these experiments would be to develop a mathematical model that incorporates the interaction between transport effects (convection and diffusion) and chemical reactions. The chemical reactions we build into the model is water-rock interaction in terms of dissolution/precipitation of minerals and aqueous chemistry under the assumption of thermodynamical equilibrium. The model should be general enough to possibly give insight into more complicated systems relevant for study of chalk weakening effects.

1.2. **The model.** Let Ω be the domain of calcite $CaCO_3$ and define the molar concentrations of the different species in the units of mol/liter:

$\rho_c = [CaCO_3]$ (solid)	$\rho_{ca} = [Ca^{2+}]$ (ions)	$\rho_h = [H^+]$ (ions)
$\rho_g = [CaSO_4]$ (solid)	$\rho_{mg} = [Mg^{2+}]$ (ions)	$\rho_{oh} = [OH^-]$ (ions)
$\rho_m = [MgCO_3]$ (solid)	$\rho_{so} = [SO_4^{2-}]$ (ions)	$\rho_{hco} = [HCO_3^-]$ (ions)
$\rho_l = [H_2O]$ (water)	$\rho_{na} = [Na^+]$ (ions)	$\rho_{co} = [CO_3^{2-}]$ (ions)
	$\rho_{cl} = [Cl^-]$ (ions)	

The domain Ω itself may depend on time, due to the undergoing chemical reactions which affect its surface. Currently, we neglect this dependence. Since we are including the bulk volume (matrix volume + pore volume) in the definition of the above densities, we will call them *total concentrations*. Later we shall define *porous concentrations* when dealing with porosity.

The primary unknown concentrations are ρ_c, ρ_g, ρ_m, ρ_l, ρ_{ca}, ρ_{so}, ρ_{mg}, ρ_{na}, ρ_{cl}, ρ_h, ρ_{oh}, ρ_{co}, and ρ_{hco}. We shall assume that the Na^+ and Cl^- ions do not take part in the chemical reactions, i.e., their concentrations ρ_{na} and ρ_{cl} are determined by the transport mechanisms only (injection rate and molecular diffusion). We include chemical kinetics associated with the concentrations ρ_c, ρ_g, ρ_m, ρ_{ca}, ρ_{so}, ρ_{mg} involved in the water-rock interactions (dissolution/precipitation), whereas the concentrations ρ_h, ρ_{oh}, ρ_{co}, and ρ_{hco} involved in the aqueous chemistry, are obtained by considering equilibrium state equations. In addition, a charge balance equation is included for the ions in question.

Water-rock interaction (dissolution and precipitation). The aim is to develop a single mathematical model that can take into account important aspects of the full behavior as observed from various laboratory experiments and briefly described in Section 1.1. The model represents a reactive transport system with three mineral phases ($CaCO_3$, $CaSO_4$, $MgCO_3$) and three aqueous species (Ca^{2+}, SO_4^{2-}, Mg^{2+}) which react according to basic kinetic laws. More precisely, the chemical reactions we want to include are:

$$CaCO_3(s) + H^+ \rightleftharpoons Ca^{2+} + HCO_3^- \qquad \text{(dissolution/precipitation)}, \tag{1}$$

$$CaSO_4(s) \rightleftharpoons Ca^{2+} + SO_4^{2-} \qquad \text{(dissolution/precipitation)}, \tag{2}$$

$$MgCO_3(s) + H^+ \rightleftharpoons Mg^{2+} + HCO_3^- \qquad \text{(dissolution/precipitation)}. \tag{3}$$

We shall include reaction kinetic relevant for these processes.

Aqueous chemistry (chemical reactions in the liquid phase). Chemical reactions in the liquid phase are assumed to be at equilibrium. More precisely, in addition to (1)–(3), we will also make use of the following chemical reactions in order to determine concentrations of HCO_3^-, H^+, CO_3^{2-} and OH^- (which are species in the water phase):

$$CO_2(g) + H_2O \rightleftharpoons HCO_3^- + H^+, \tag{4}$$

$$HCO_3^- \rightleftharpoons CO_3^{2-} + H^+, \tag{5}$$

$$H_2O \rightleftharpoons OH^- + H^+. \tag{6}$$

We do not include reaction kinetic associated with these chemical reactions but assume that they are at equilibrium. In other words, it is implicitly assumed that they take place at a much faster time scale than the dissolution/precipitation processes (1)–(3). As mentioned, we shall also include a charge balance equation. In

particular, the concentration of Na^+ and Cl^-, if present, is included in this relation, hence, indirectly will have an impact on the dissolution/precipitation processes.

Model for transport of aqueous species coupled with precipitation and dissolution of minerals. The core plug under consideration is initially filled with formation water. At initial time the formation water is in equilibrium with the minerals attached to the rock inside the core. Then a brine, which contains known concentrations of various ions, is injected into the core. Hence, there will be a transport of the different ions due to a combination of convective and diffusive forces. This creates concentration fronts that move with a certain speed. At these fronts, as well as behind them, chemical reactions will take place, both within the aqueous phase as well as on the rock surface. Of particular interest for us is to gain some insight into the relation between the concentrations of various ions in water, respectively, at the outlet and at the inlet. For that purpose it is necessary to study the interaction between transport, chemical reaction, and the properties of the porous media (like porosity and permeability). We follow along the line of previous studies, see for example [1, 2, 3], and formulate a one-dimensional model. More precisely, we shall in this work deal with a model of the following form:

$$\begin{aligned}
\partial_t(\phi C_{na}) + \partial_x(JC_{na}) &= \partial_x(D_m\phi\partial_x C_{na}),\\
\partial_t(\phi C_{cl}) + \partial_x(JC_{cl}) &= \partial_x(D_m\phi\partial_x C_{cl}),\\
\partial_t(\phi C_{ca}) + \partial_x(JC_{ca}) &= \partial_x(D_m\phi\partial_x C_{ca}) + \tau(\dot r_c + \dot r_g),\\
\partial_t(\phi C_{so}) + \partial_x(JC_{so}) &= \partial_x(D_m\phi\partial_x C_{so}) + \tau\dot r_g,\\
\partial_t(\phi C_{mg}) + \partial_x(JC_{mg}) &= \partial_x(D_m\phi\partial_x C_{mg}) + \tau\dot r_m,\\
\partial_t\rho_c &= -\tau\dot r_c,\\
\partial_t\rho_g &= -\tau\dot r_g,\\
\partial_t\rho_m &= -\tau\dot r_m,\\
\partial_x J = \frac{\tau}{C}(\dot r_c + 2\dot r_g + \dot r_m), &\qquad J = -\varepsilon\kappa\partial_x p, \qquad \varepsilon = \frac{\overline{\kappa}\,\overline{p}}{\nu\overline{D}_m}.
\end{aligned} \tag{7}$$

All the details leading to this model are given in Section 2 and 3. Here we just note that $\overline{\kappa}$, $\overline{p}$, and $\overline{D}_m$, respectively, are characteristic permeability, pressure, and molecular diffusion coefficient, whereas ν is the viscosity assumed to be constant. κ, p, and D_m represent corresponding dimensionless quantities. In the model (7), a characteristic time τ and length scale $L = \sqrt{\overline{D}_m\tau}$ have also been introduced. The unknown variables we solve for are C_{na}, C_{cl}, C_{ca}, C_{so}, C_{mg}, ρ_c, ρ_g, ρ_m (in terms of mole per liter), and pressure p. Moreover, we must specify rate equations $\dot r_k = \dot r_k(\rho_{ca}, \rho_{so}, \rho_{mg}, \rho_{na}, \rho_{cl})$ for $k = c, g, m$. More precisely, the reaction terms take the form

$$\begin{aligned}
\dot r_c &= k_1^c\Big[\mathrm{sgn}^+(\rho_c)F_c^+(\rho_{ca}, \rho_{so}, \rho_{mg}, \rho_{na}, \rho_{cl}) - F_c^-(\rho_{ca}, \rho_{so}, \rho_{mg}, \rho_{na}, \rho_{cl})\Big],\\
\dot r_g &= k_1^g\Big[\mathrm{sgn}^+(\rho_g)F_g^+(\rho_{ca}, \rho_{so}, \rho_{mg}, \rho_{na}, \rho_{cl}) - F_g^-(\rho_{ca}, \rho_{so}, \rho_{mg}, \rho_{na}, \rho_{cl})\Big],\\
\dot r_m &= k_1^m\Big[\mathrm{sgn}^+(\rho_m)F_m^+(\rho_{ca}, \rho_{so}, \rho_{mg}, \rho_{na}, \rho_{cl}) - F_m^-(\rho_{ca}, \rho_{so}, \rho_{mg}, \rho_{na}, \rho_{cl})\Big],
\end{aligned} \tag{8}$$

where the functions F_c, F_g, and F_m represent the kinetics of the precipitation and dissolution processes in question and k_1^c, k_1^g, and k_1^m are corresponding reaction rate constants. Here $F_I = F_I^+ - F_I^-$, $I = c, g, m$, is a decomposition of F into its positive and negative parts, whereas $\mathrm{sgn}(x)^+ = 1$ if $x > 0$, otherwise it is 0.

$F_I < 0$ represents precipitation, whereas $F_I > 0$ represents dissolution. The above formulation takes into account that a mineral can be dissolved only as long as it exists, and is similar to what has been done in other works, see for example [8, 42] and references therein.

C_k represents *porous* concentrations and are related to the total concentrations by $\rho_k = \phi C_k$, for $k = ca, so, mg, na, cl$. C represents the sum of the water concentration and the total concentration of the various aqueous species, and it is assumed that C is constant, i.e., incompressible fluid. We shall also, as a first step, assume that J is constant. This is reasonable in view of the last equation (left) of (7) since, typically, $C \gg \tau(\dot{r}_c + 2\dot{r}_g + \dot{r}_m)$.

Porosity ϕ and permeability κ are taken to be constant in the numerical calculations in Section 5. More generally, it would be reasonable to let, for example, porosity depend on the mineral composition determined by ρ_c, ρ_g, ρ_m, similar to what has been done in [1, 2, 3] for a simpler system relevant for the study of chemical aggression to calcium carbonate stones. See also [11], and references therein, for a model where porosity and permeability are non-constant.

1.3. **Main objectives of the paper.** The aim of this paper is as follows:

- Develop a model that is general enough to describe water-rock interactions relevant for chalk weakening effects associated with carbonate reservoirs.
- Provide a first evaluation of the model by comparing calculated ion concentrations with corresponding concentration profiles measured experimentally at the outlet of core samples for a simplified brine composed of water and $MgCl_2$.
- Gain some basic insight into characteristic features of the model. The main tool in this paper for that purpose is the use of an appropriate discrete version of the model. We base the model on known parameters and use it to infer insight into quantitative behavior that is not easy to measure, like in situ concentrations. In particular, we focus on issues like
  - the balance between dissolution/precipitation and transport effects;
  - how to transfer insight from experimental studies on core plugs to a larger scale relevant for reservoir flow (upscaling).

The structure of this paper is as follows: In Section 2 we describe the equations relevant for the aqueous equilibrium chemistry represented by (4)–(6), as well as non-equilibrium chemistry (dissolution/precipitation) represented by (1)–(3). In Section 3 we extend the model by incorporating convective and diffusive effects. Then, in Section 4 we briefly describe a numerical method for solving the resulting model (7) and (8) based on operator splitting. Finally, in Section 5 we provide a first evaluation of the model by computing solutions for a case where experimental data have recently been obtained. Further numerical experiments are included to shed light on characteristic behavior of the model.

1.4. **A review of some relevant studies.** It is instructive to try to put the model (7) and (8) into perspective by briefly reviewing previous works on similar type of models. In [9] a simplified diffusion-reaction model relevant for precipitation/dissolution processes is studied in N-dimensions. The form of the model in 1D is

$$u_t - u_{xx} = -\lambda G(u, v), \qquad w_t = \lambda G(u, v), \tag{9}$$

where u is the concentration of an aqueous species and moves due to molecular diffusion, and w stands for the concentration of a mineral phase. $G(u, v)$ represents the reaction rate and models either precipitation or dissolution, and λ is a constant rate. Such models for water-rock interactions are relevant for the study of radioactive waste storage, oil industry problems like chalk weakening, and CO_2 storage.

In [9] main focus is on the existence of weak solutions of (9) and the limiting behavior of the solution (in a precise mathematical sense) as the kinetic rate λ tends to infinity. In other words, one tries to obtain a model that represents this thermodynamical equilibrium solution. In [8] a slightly more complicated system composed of two aqueous species and one mineral phase is considered. A numerical discretization is discussed and employed to show existence of weak solutions. A special characteristic and challenge of these models is the discontinuous reaction term of unknown sign (depending on either precipitation or dissolution). See also [42] for similar results for a 1D model of the form (9) and [22] for the same kind of model, however, whose reaction term does not change sign. A nonlinear version of this model is studied in [23] whereas a reaction-diffusion system with two mobile reactants are studied in [7].

Effective discretization algorithms for solving complex diffusion-dissolution and precipitation chemical system of equations constituted of partial differential equations (PDE) and ordinary differential equations (ODE) with nonlinear discontinuous right hand side, is investigated in [20]. The approach is based on an operator splitting method alternating between solving a system of pure diffusion equations and a system of stiff ODEs. Special attention is paid to the ODEs with possible jumping nonlinearities. Operator splitting methods are known to provide cheap and high order approximations to reaction-diffusion equations [15, 16, 45, 31, 27]. In [38, 13] a class of semi-implicit schemes is explored, which treats the linear diffusions exactly and explicitly, and the nonlinear reactions implicitly. A distinctive feature of the scheme is the decoupling between the exact evolution of the diffusion terms and implicit treatment of the nonlinear reaction terms.

We have already mentioned the works [1, 2, 3] which deal with systems relevant for the study of chemical aggression to calcium carbonate stones. Reliable numerical schemes are derived and explored as well as asymptotic behavior of the model in question as time goes to infinity or reaction rate goes to infinity. The evolution of damage in a specimen of homogeneous material under the effect of mechanical stress and chemical aggressions is studied in [37, 40]. The model that is formulated allows for studying the damage evolution as a blow-up problem. See also [5, 6] for similar type of studies where focus is on fluid flow and damage accumulation.

There is a very active research field within theoretical biology where systems of convection-diffusion-reaction equations are derived. Numerical and analytical solutions are often studied in simplified 1D geometries and comparisons with experimental data are made. As an example of this type of work we refer the readers to [14] dealing with cell dynamics. Analytical traveling wave solutions are obtained and used for predicting how the speed of the cell depends on various central parameters. Another model, similar to (9), is studied in [24, 25]. Wellposedness properties of the model, relevant for invasion of bacteria in wounds, is studied in the first work, as well as convergence to a Stefan-like boundary problem as the "reaction" rate tends to infinity. Traveling wave analysis is carried out in the second work demonstrating existence of such solutions subject to appropriate conditions. Further inspiration

can be found in the works [34, 35] which explore traveling wave solutions for a model of malignant invasion in the study of cell dynamics. The model is a 1D three-equation model, composed of one diffusion-reaction type of equation and two ODEs. These equations are coupled through reaction terms as well as nonlinear coefficients. See also [46] for a an interesting work for a similar type of model and [44] for a nice overview of mathematical models describing the growth of avascular tumors.

Finally, we would like to mention some interesting works by van Duijn and coworkers [28, 19] where a model of the form

$$(u+v)_t + qu_x - Du_{xx} = 0, \qquad v_t = k(g(u;c) - wK),$$

is studied. Here u represents aqueous species, v mineral phase, and w is a third unknown which is used to take into account the nature of the dissolution reaction. Moreover, q and D are constant pore velocity and molecular diffusion coefficient, respectively. The dissolution/precipitation is described by $g(u;c)$, K is the saturation constant, and k the rate of the chemical reaction. c represents the excess charge distribution and may be set to be constant or to satisfy a convection-diffusion equation. In [28] traveling wave solutions are constructed under the assumption that c is constant for the following different cases: (i) non-equilibrium reactions ($k < \infty$) with diffusion; (ii) equilibrium reactions ($k = \infty$) with diffusion; (iii) non-equilibrium reactions where diffusion is neglected. In [19] explicit solutions of Riemann problems are constructed for the case where diffusion D is zero and (i) infinitely fast kinetic is assumed ($k = \infty$) so that $g(u;c) = wK$; (ii) finitely rate constant k is used such that the solutes are not in equilibrium but is kinetically controlled. The construction of analytical (semi-analytical) solutions as discussed in these works probably is relevant for the study of the model (7) and (8) as such techniques can enhance the understanding of the interplay convection-diffusion-chemical reactions. Hopefully such techniques also can be employed to provide solutions for validating numerical solutions of appropriate simplified versions of the model (7) and (8).

2. Derivation of the model without transport effects.

2.1. Dissolution/precipitation.

For equilibrium processes of the general form

$$\mathrm{A} + \mathrm{B} \rightleftharpoons \mathrm{X} + \mathrm{Y}, \tag{10}$$

we have that the reaction rate $\dot{r}$ (assuming they each are elementary) can be expressed as:

$$\dot{r} = k_1[A][B] - k_{-1}[X][Y], \tag{11}$$

where k_1 is the rate coefficient for the reaction which consumes A and B whereas k_{-1} is the rate coefficient for the backward reaction which consumes X and Y and produces A and B. In the following, the concentration $[I]$ of a substance I is given in mol/liter. For the chemical reactions (1)–(3), k_1 represents *dissolution* of minerals whereas k_{-1} represents *precipitation*. The unit of $\dot{r}$ is $(\text{mol/liter})s^{-1}$. The constants k_1 and k_{-1} are related to the equilibrium coefficient K for the reaction in question by the following relationship, obtained by setting $\dot{r} = 0$ in (11):

$$K \overset{\text{def}}{:=} \frac{k_1}{k_{-1}} = \frac{[X][Y]}{[A][B]}. \tag{12}$$

This constant is often referred to as the *solubility product* and is typically a known constant. Furthermore, for the rate $\dot{r}$ associated with the chemical reaction (10),

we have

$$\dot{r} = -\frac{1}{V}\frac{dn_A}{dt} = -\frac{1}{V}\frac{dn_B}{dt} = \frac{1}{V}\frac{dn_X}{dt} = \frac{1}{V}\frac{dn_Y}{dt}, \tag{13}$$

where n_I represents the number of moles of substance $I = A, B, X, Y$ per unit volume V. Using the relation that $[I] = n_I/V$ for $I = A, B, X, Y$, we can write (13) in the form

$$\dot{r} = -\frac{d[A]}{dt} = -\frac{d[B]}{dt} = \frac{d[X]}{dt} = \frac{d[Y]}{dt}. \tag{14}$$

Remark 1. Note that the rate coefficients k_1 and k_{-1} may depend on various information relevant for the specific chemical reactions under consideration. Examples of this kind of information include temperature, pressure, activation energy (ionic strength), area of grain surface, etc. In this work, we shall treat the rate coefficients as constants.

2.2. **Rate equations for the chemical processes involved.** The form of the chemical reaction terms $\dot{r}_i$, for $i = c, g, m$ follows from Section 2.1. Note that in the following we have tactically assumed that the chemical reactions take place in an ideal solution since we do not distinguish between *concentration* and *chemical activity*. The inclusion of activity is given in Section 2.7. We also implicitly have assumed that all three minerals always are present. The general case where one or several of the minerals vanish or do not exist initially, is accounted for in Section 2.3. Based on (11) we get the following rate equations associated with the minerals ρ_c, ρ_g, and ρ_m as described by (1)–(3):

$$\dot{r}_c = k_1^c\rho_h - k_{-1}^c\rho_{ca}\rho_{hco} = k_1^c\Big(\rho_h - \frac{\rho_{hco}\rho_{ca}}{K^c}\Big) = k_1^c F_c(\rho_{ca}, \rho_{so}, \rho_{mg}; \rho_{na}, \rho_{cl}), \tag{15}$$

$$\dot{r}_g = k_1^g - k_{-1}^g\rho_{ca}\rho_{so} = k_1^g\Big(1 - \frac{\rho_{ca}\rho_{so}}{K^g}\Big) = k_1^g F_g(\rho_{ca}, \rho_{so}, \rho_{mg}; \rho_{na}, \rho_{cl}), \tag{16}$$

$$\dot{r}_m = k_1^m\rho_h - k_{-1}^m\rho_{mg}\rho_{hco} = k_1^m\Big(\rho_h - \frac{\rho_{hco}\rho_{mg}}{K^m}\Big) = k_1^m F_m(\rho_{ca}, \rho_{so}, \rho_{mg}; \rho_{na}, \rho_{cl}), \tag{17}$$

where

$$K^c = \frac{k_1^c}{k_{-1}^c}, \qquad K^g = \frac{k_1^g}{k_{-1}^g}, \qquad K^m = \frac{k_1^m}{k_{-1}^m}, \tag{18}$$

and the functions F_c, F_g, and F_m, are defined by (15)–(17). Here we have used that the ion activity of a solid component (the minerals) is set to one, see for example [8], i.e. we have set $\rho_c = \rho_g = \rho_m = 1$ in (15)–(17). k_{-1}^j represents the rate of precipitation whereas k_1^j represents the rate of dissolution associated with the different minerals $j = c, g, m$ corresponding to $CaCO_3$, $CaSO_4$, and $MgCO_3$. Similarly, K^j is used to represent the equilibrium constant associated with $j = c, g, m$. These are known values. On the other hand, typically much less is known about the rate of precipitation/dissolution represented by k_1^j and k_{-1}^j.

Applying (14) for the general process (10), we get the following rate equations associated with the minerals ρ_c, ρ_g, and ρ_m:

$$\begin{aligned}
\frac{d\rho_c}{dt} &= -\dot{r}_c = -k_1^c\Big(\rho_h - \frac{\rho_{hco}\rho_{ca}}{K^c}\Big),\\
\frac{d\rho_g}{dt} &= -\dot{r}_g = -k_1^g\Big(1 - \frac{\rho_{ca}\rho_{so}}{K^g}\Big),\\
\frac{d\rho_m}{dt} &= -\dot{r}_m = -k_1^m\Big(\rho_h - \frac{\rho_{hco}\rho_{mg}}{K^m}\Big).
\end{aligned} \tag{19}$$

Similarly, in view of the chemical reactions (2) and (3), respectively, we can apply (14) and directly put up rate equations for SO_4^{2-} and Mg^{2+} of the form

$$\begin{aligned} \frac{d\rho_{so}}{dt} &= \dot{r}_{so} = \dot{r}_g = k_1^g\Big(1 - \frac{\rho_{ca}\rho_{so}}{K^g}\Big), \\ \frac{d\rho_{mg}}{dt} &= \dot{r}_{mg} = \dot{r}_m = k_1^m\Big(\rho_h - \frac{\rho_{hco}\rho_{mg}}{K^m}\Big). \end{aligned} \tag{20}$$

Finally, we see that Ca^{2+} is involved in both reaction (1) and (2). Thus, we might consider these two chemical reactions as parallel or competitive reactions. In other words, the rate associated with Ca^{2+} should be the sum of the rates $\dot{r}_c$ and $\dot{r}_g$.

$$\frac{d\rho_{ca}}{dt} = \dot{r}_{ca} = \dot{r}_c + \dot{r}_g = k_1^c\Big(\rho_h - \frac{\rho_{hco}\rho_{ca}}{K^c}\Big) + k_1^g\Big(1 - \frac{\rho_{ca}\rho_{so}}{K^g}\Big). \tag{21}$$

Here we remark that ρ_h and ρ_{hco} are nonlinear functions of the form

$$\rho_h = \rho_h(\rho_{ca}, \rho_{mg}, \rho_{so}; \rho_{na}, \rho_{cl}), \qquad \rho_{hco} = \rho_{hco}(\rho_{ca}, \rho_{mg}, \rho_{so}; \rho_{na}, \rho_{cl}).$$

This follows by assuming that the chemical reactions (4)–(6), relevant for the aqueous chemistry, is much faster than the dissolution/precipitation processes described by (1)–(3). Details are given in Section 2.5 as described by (35), (33), and (27).

Remark 2. So far we have followed a rather common practice [8, 30] and assumed that the activity of aqueous species is given by its concentration when we formulate rate equations. More generally, it might be important to deal with chemical activity in the rate equations by taking into account the relation

$$a = \gamma\rho,$$

where γ is the activity coefficient, a is activity, and ρ is density. This will be done in Section 2.7 and is used for the numerical calculations in Section 5.

Remark 3. Note that the functional form of the reaction terms given by (19)–(21) should be considered representative, rather than cast in stone. Typically, most of the rate laws devised for mineral dissolution and precipitation are more empirical than theoretical, since the reaction mechanism is unknown. As remarked in [8], the determination of rates is a topic for intensive research within the geochemical community [30] in the lack of a general theory of surface dissolution/precipitation mechanisms. In particular, other functional forms should be explored as we gain more insight into the kinetics associated with the chemical reactions (1)–(3).

Remark 4. In the proposed model for the chemical reactions we have not at this stage included adsorption or ion exchange processes on the surface of the rock, see for example [17, 18]. Focus is on fluid-rock interactions in terms of dissolution and precipitation.

2.3. **A modified model.** An important modification is to take into account the fact that mineral dissolution stops once the mineral has disappeared [8, 36]. To build this mechanism into the rate equations given by (15)–(17), we change these equations in the following manner

$$\begin{aligned} \dot{r}_c &= k_1^c\Big[\mathrm{sgn}^+(\rho_c)F_c^+(\rho_{ca}, \rho_{so}, \rho_{mg}) - F_c^-(\rho_{ca}, \rho_{so}, \rho_{mg})\Big], \\ \dot{r}_g &= k_1^g\Big[\mathrm{sgn}^+(\rho_g)F_g^+(\rho_{ca}, \rho_{so}, \rho_{mg}) - F_g^-(\rho_{ca}, \rho_{so}, \rho_{mg})\Big], \\ \dot{r}_m &= k_1^m\Big[\mathrm{sgn}^+(\rho_m)F_m^+(\rho_{ca}, \rho_{so}, \rho_{mg}) - F_m^-(\rho_{ca}, \rho_{so}, \rho_{mg})\Big], \end{aligned} \tag{22}$$

where

$$\mathrm{sgn}^+(x) = \begin{cases} 1, & \text{if } x \geq 0; \\ 0, & \text{otherwise,} \end{cases}$$
$$F_I = F_I^+ - F_I^-, \quad \text{where} \quad F_I^+ = \max(0, F_I), \quad F_I^- = \max(0, -F_I).$$

Clearly, in view of (19), we see that for $F_I < 0$ where $I = c, g, m$ represents the mineral in question, the mineral precipitates; for $F_I = 0$ chemical equilibrium exists and nothing happens; for $F_I > 0$ the mineral dissolves, but only as long as the mineral exists, i.e., $\rho_I > 0$. Using (22) the resulting system now takes the following form for the minerals

$$\begin{aligned} \frac{d\rho_c}{dt} &= -\dot{r}_c = -k_1^c \Big[\mathrm{sgn}^+(\rho_c) F_c^+(\cdot) - F_c^-(\cdot) \Big], \\ \frac{d\rho_g}{dt} &= -\dot{r}_g = -k_1^g \Big[\mathrm{sgn}^+(\rho_g) F_g^+(\cdot) - F_g^-(\cdot) \Big], \\ \frac{d\rho_m}{dt} &= -\dot{r}_m = -k_1^m \Big[\mathrm{sgn}^+(\rho_m) F_m^+(\cdot) - F_m^-(\cdot) \Big], \end{aligned} \tag{23}$$

and for the aqueous species

$$\begin{aligned} \frac{d\rho_{ca}}{dt} &= \dot{r}_{ca} = \dot{r}_c + \dot{r}_g = k_1^c \Big[\mathrm{sgn}^+(\rho_c) F_c^+(\cdot) - F_c^-(\cdot) \Big] + k_1^g \Big[\mathrm{sgn}^+(\rho_g) F_g^+(\cdot) - F_g^-(\cdot) \Big], \\ \frac{d\rho_{so}}{dt} &= \dot{r}_{so} = \dot{r}_g = k_1^g \Big[\mathrm{sgn}^+(\rho_g) F_g^+(\cdot) - F_g^-(\cdot) \Big], \\ \frac{d\rho_{mg}}{dt} &= \dot{r}_{mg} = \dot{r}_m = k_1^m \Big[\mathrm{sgn}^+(\rho_m) F_m^+(\cdot) - F_m^-(\cdot) \Big]. \end{aligned} \tag{24}$$

2.4. **Kinetics associated with the fluid-rock interaction.** In a more complete description we also will take into account convective and diffusive forces associated with the brine in the pore space. In order to include such effects we must consider the following equations for the total concentrations ρ_c, ρ_g, ρ_m, ρ_l, ρ_{ca}, ρ_{so}, ρ_{mg}, ρ_{na}, ρ_{cl}:

$$\begin{aligned} \partial_t \rho_l + \nabla \cdot (\rho_l \mathbf{v}_l) &= 0, && \text{(water flowing through the pore space)} \\ \partial_t \rho_{na} + \nabla \cdot (\rho_{na} \mathbf{v}_g) &= 0, && (\mathrm{Na}^+\text{-ions in water}) \\ \partial_t \rho_{cl} + \nabla \cdot (\rho_{cl} \mathbf{v}_g) &= 0, && (\mathrm{Cl}^-\text{-ions in water}) \\ \partial_t \rho_{ca} + \nabla \cdot (\rho_{ca} \mathbf{v}_g) &= \dot{r}_c + \dot{r}_g, && (\mathrm{Ca}^{2+}\text{-ions in water}) \\ \partial_t \rho_{so} + \nabla \cdot (\rho_{so} \mathbf{v}_g) &= \dot{r}_g, && (\mathrm{SO}_4^{2-}\text{-ions in water}) \\ \partial_t \rho_{mg} + \nabla \cdot (\rho_{mg} \mathbf{v}_g) &= \dot{r}_m, && (\mathrm{Mg}^{2+}\text{-ions in water}) \\ \partial_t \rho_c &= -\dot{r}_c, && \text{(precipitation/dissolution of } \mathrm{CaCO_3}) \\ \partial_t \rho_g &= -\dot{r}_g, && \text{(precipitation/dissolution of } \mathrm{CaSO_4}) \\ \partial_t \rho_m &= -\dot{r}_m, && \text{(precipitation/dissolution of } \mathrm{MgCO_3}). \end{aligned} \tag{25}$$

The first six equations represent concentrations associated with the pore space, the last three equations are associated with the matrix. Here $\mathbf{v}_l$ and $\mathbf{v}_g$ are, respectively, the water and ion "fluid" velocities. In the rest of this section we shall focus on the simplified model where convective and diffusive forces are neglected and main focus

is on the reaction kinetic. That is, the model takes the form

$$\begin{aligned} &\frac{d\rho_l}{dt} = 0, && \frac{d\rho_{na}}{dt} = 0, && \frac{d\rho_{cl}}{dt} = 0, \\ &\frac{d\rho_{ca}}{dt} = \dot{r}_c + \dot{r}_g, && \frac{d\rho_{so}}{dt} = \dot{r}_g, && \frac{d\rho_{mg}}{dt} = \dot{r}_m, \\ &\frac{d\rho_c}{dt} = -\dot{r}_c, && \frac{d\rho_g}{dt} = -\dot{r}_g, && \frac{d\rho_m}{dt} = -\dot{r}_m. \end{aligned} \tag{26}$$

Later, in Section 3, we shall develop the full model where convection and molecular diffusion is taken into account. This stepwise approach is reasonable in view of the fact that we shall use an operator splitting approach where we switch between solving (i) the submodel (26); (ii) the submodel obtained by setting the right hand side in (25) to zero.

From (26) we calculate the concentrations $\rho_l, \rho_{na}, \rho_{cl}, \rho_{ca}, \rho_{so}, \rho_{mg}, \rho_c, \rho_g$, and ρ_m. What remains then is to determine the concentrations ρ_h, ρ_{hco}, and ρ_{oh}, ρ_{co}, which we need for the evaluation of the reaction terms F_c, F_g, and F_m in (23) and (24). For that purpose we shall apply equilibrium considerations associated with the chemical reactions (4)–(6), thereby implicitly assuming that these reactions are much faster than the precipitation/dissolution processes (1)–(3).

2.5. **Aqueous chemistry.** In the following, we assume that we know the distribution of the concentrations ρ_{na} and ρ_{cl} determined from the second and third equation of (25). Based on this, we shall discuss the various equations associated with the chemical reactions described by (4)–(6). First, we shall assume that the CO_2 partial pressure P_{CO_2} is known, from which the CO_2 concentration can be determined. More precisely, the local equilibrium associated with (4) gives the relation

$$C_1 = P_{CO_2} K = \rho_{hco}\rho_h, \tag{27}$$

for an appropriate choice of the equilibrium constant (solubility product) K and partial pressure P_{CO_2}. The chemical reaction equation (5) gives us

$$C_2 = \frac{\rho_{co}\rho_h}{\rho_{hco}}, \tag{28}$$

where C_2 is a known solubility constant. Similarly, from (6), we also have the basic relation for ρ_h and ρ_{oh}

$$C_w = \rho_h \rho_{oh}, \tag{29}$$

where C_w is known. Moreover, the following aqueous *charge balance equation* should hold for the various species contained in the water

$$\sum_i \rho_i Z_i = 0, \tag{30}$$

where Z_i refers to the ionic charge of species i. For the system in question, this results in the following balance equation:

$$2\rho_{ca} + 2\rho_{mg} + \rho_h + \rho_{na} = 2\rho_{so} + \rho_{hco} + 2\rho_{co} + \rho_{oh} + \rho_{cl}. \tag{31}$$

Thus, (27)–(30) gives us four equations that allow us to solve for ρ_h, ρ_{hco}, ρ_{co}, and ρ_{oh}. In particular, the relation (31) can be written in the form

$$C_3 = \rho_{hco} + 2\rho_{co} + \rho_{oh} - \rho_h, \tag{32}$$

where

$$C_3 = C_3(\rho_{ca}, \rho_{mg}, \rho_{so}; \rho_{na}, \rho_{cl}) = 2(\rho_{ca} + \rho_{mg} - \rho_{so}) + (\rho_{na} - \rho_{cl}). \tag{33}$$

This relation can then be rewritten in the form

$$C_3 = \rho_{hco} + 2C_2\frac{\rho_{hco}}{\rho_h} + \frac{C_w}{\rho_h} - \rho_h, \tag{34}$$

where we have used (28) and (29). Combining (27) and (34) we get

$$C_3 = \frac{C_1 + C_w}{\rho_h} + \frac{2C_1C_2}{\rho_h^2} - \rho_h,$$

which can be rewritten as a third order polynomial in terms of ρ_h

$$\rho_h^3 + C_3\rho_h^2 - (C_1 + C_w)\rho_h - 2C_1C_2 = 0. \tag{35}$$

We shall in the following make use of the simplifying assumption that the concentration ρ_{co} of CO_3^{2-} is low for pH in the range $[6, 8]$ and, thus, can be neglected in the charge balance equation (31). Consequently, instead of (32) we consider

$$C_3 = \rho_{hco} + \rho_{oh} - \rho_h, \tag{36}$$

where C_3 still is given by (33). This simplification implies that (35) is replaced by the the second order equation $\rho_h^2 + C_3\rho_h - (C_1 + C_w) = 0$, which gives

$$\rho_h = \frac{1}{2}\Big(-C_3 + \sqrt{C_3^2 + 4(C_1 + C_w)}\Big), \qquad \rho_{hco} = \frac{C_1}{\rho_h}. \tag{37}$$

Finally, ρ_{co} and ρ_{oh} can be determined from the equations (28) and (29). We note that $\rho_h = \rho_h(\rho_{ca}, \rho_{so}, \rho_{mg}; \rho_{na}, \rho_{cl})$, in view of (33). Now it is timely to recall the expressions for F_c, F_g, and F_m:

$$\begin{aligned}
F_c(\rho_{ca}, \rho_{so}, \rho_{mg}) &= \Big(\rho_h - \frac{\rho_{hco}\rho_{ca}}{K^c}\Big) = \Big(\rho_h - \frac{\rho_{ca}C_1}{\rho_h K^c}\Big),\\
F_g(\rho_{ca}, \rho_{so}) &= \Big(1 - \frac{\rho_{ca}\rho_{so}}{K^g}\Big) = \Big(1 - \frac{\rho_{ca}\rho_{so}}{K^g}\Big),\\
F_m(\rho_{ca}, \rho_{so}, \rho_{mg}) &= \Big(\rho_h - \frac{\rho_{hco}\rho_{mg}}{K^m}\Big) = \Big(\rho_h - \frac{\rho_{mg}C_1}{\rho_h K^m}\Big).
\end{aligned} \tag{38}$$

2.6. **Transient solutions with no convective and diffusive effects included.** In view of (26) we get

$$\begin{aligned}
&\frac{d\rho_g}{dt} + \frac{d\rho_{so}}{dt} = -\dot r_g + \dot r_{so} = 0, \qquad \frac{d\rho_m}{dt} + \frac{d\rho_{mg}}{dt} = -\dot r_m + \dot r_{mg} = 0,\\
&\frac{d\rho_c}{dt} + \frac{d\rho_{ca}}{dt} - \frac{d\rho_{so}}{dt} = -\dot r_c + \dot r_{ca} - \dot r_{so} = 0,
\end{aligned}$$

where ρ_l, ρ_{na} and ρ_{cl} are known quantities. Thus, we can write the system (26) in the form

$$\begin{aligned}
&\frac{d\rho_{ca}}{dt} = \dot r_c + \dot r_g, \qquad \frac{d\rho_{so}}{dt} = \dot r_g, \qquad \frac{d\rho_{mg}}{dt} = \dot r_m, \qquad \frac{d\rho_c}{dt} = -\dot r_c,\\
&\frac{d}{dt}\Big(\rho_g + \rho_{so}\Big) = 0, \qquad \frac{d}{dt}\Big(\rho_m + \rho_{mg}\Big) = 0, \qquad \frac{d}{dt}\Big(\rho_c + \rho_{ca} - \rho_{so}\Big) = 0.
\end{aligned} \tag{39}$$

This is equivalent to

$$\begin{aligned}
\rho_g(t) &= (\rho_{g,0} + \rho_{so,0}) - \rho_{so}(t),\\
\rho_m(t) &= (\rho_{m,0} + \rho_{mg,0}) - \rho_{mg}(t),\\
\rho_c(t) &= (\rho_{c,0} + \rho_{ca,0} - \rho_{so,0}) - (\rho_{ca}(t) - \rho_{so}(t)),\\
\frac{d\rho_{ca}}{dt} &= [\dot{r}_c + \dot{r}_g](\rho_c, \rho_{ca}, \rho_{so}, \rho_{mg}),\\
\frac{d\rho_{so}}{dt} &= \dot{r}_g(\rho_g, \rho_{ca}, \rho_{so}, \rho_{mg}),\\
\frac{d\rho_{mg}}{dt} &= \dot{r}_m(\rho_m, \rho_{ca}, \rho_{so}, \rho_{mg}),
\end{aligned} \tag{40}$$

where we have suppressed the dependence on ρ_{na} and ρ_{cl} in the reaction terms since these are known constants. In other words, we have got a simplified model of the form

$$\begin{aligned}
\frac{d\rho_{ca}}{dt} &= k_1^c\Big[\mathrm{sgn}^+(\rho_c)F_c^+(\cdot) - F_c^-(\cdot)\Big] + k_1^g\Big[\mathrm{sgn}^+(\rho_g)F_g^+(\cdot) - F_g^-(\cdot)\Big],\\
\frac{d\rho_{so}}{dt} &= k_1^g\Big[\mathrm{sgn}^+(\rho_g)F_g^+(\cdot) - F_g^-(\cdot)\Big],\\
\frac{d\rho_{mg}}{dt} &= k_1^m\Big[\mathrm{sgn}^+(\rho_m)F_m^+(\cdot) - F_m^-(\cdot)\Big],
\end{aligned} \tag{41}$$

where $\rho_c(t)$, $\rho_g(t)$, and $\rho_m(t)$ itself are functions of $\rho_{ca}, \rho_{so}, \rho_{mg}$ as given by the first three algebraic relations in (40) and the functional form of F_c, F_g, and F_m are given by (38). To sum up, let us introduce some new and simpler variables

$$x = \rho_{ca}, \quad y = \rho_{so}, \quad z = \rho_{mg}, \quad u = \rho_c, \quad v = \rho_g, \quad w = \rho_m, \quad d = \rho_{na} - \rho_{cl}. \tag{42}$$

The model (40) then takes the form

$$\begin{aligned}
\frac{dx}{dt} &= k_1^c\Big[\mathrm{sgn}^+(u)F_c^+(x,y,z) - F_c^-(x,y,z)\Big] + k_1^g\Big[\mathrm{sgn}^+(v)F_g^+(x,y,z) - F_g^-(x,y,z)\Big],\\
\frac{dy}{dt} &= k_1^g\Big[\mathrm{sgn}^+(v)F_g^+(x,y,z) - F_g^-(x,y,z)\Big],\\
\frac{dz}{dt} &= k_1^m\Big[\mathrm{sgn}^+(w)F_m^+(x,y,z) - F_m^-(x,y,z)\Big],
\end{aligned} \tag{43}$$

where

$$\begin{aligned}
u(t) &= -(x-y)(t) + (u_0 + x_0 - y_0),\\
v(t) &= -y(t) + (v_0 + y_0),\\
w(t) &= -z(t) + (w_0 + z_0),
\end{aligned} \tag{44}$$

and

$$\begin{aligned}
F_c(x,y,z) &= \Big(\rho_h(x,y,z) - \frac{xC_1}{\rho_h(x,y,z)K^c}\Big),\\
F_g(x,y,z) &= \Big(1 - \frac{xy}{K^g}\Big),\\
F_m(x,y,z) &= \Big(\rho_h(x,y,z) - \frac{zC_1}{\rho_h(x,y,z)K^m}\Big),
\end{aligned} \tag{45}$$

and

$$\rho_h(x,y,z) = \frac{1}{2}\Big(-C_3(x,y,z;d) + \sqrt{C_3(x,y,z;d)^2 + 4(C_1+C_w)}\Big), \quad \text{with} \quad C_3(x,y,z;d) = 2(x-y+z)+d. \tag{46}$$

2.7. **Inclusion of chemical activity coefficients.** A more correct modeling of the chemical reactions would be to use activities. This is taken into account in the following manner. First, we consider the model (41) where F_c, F_g, and F_m now are replaced by (see Remark 2)

$$\begin{aligned} F_c(a_{ca},a_{so},a_{mg}) &= \Big(a_h - \frac{a_{hco}a_{ca}}{K^c}\Big) = \Big(\gamma_h\rho_h - \frac{\gamma_{ca}\gamma_{hco}\rho_{ca}\rho_{hco}}{K^c}\Big), \\ F_g(a_{ca},a_{so}) &= \Big(1 - \frac{a_{ca}a_{so}}{K^g}\Big) = \Big(1 - \frac{\gamma_{ca}\gamma_{so}\rho_{ca}\rho_{so}}{K^g}\Big), \\ F_m(a_{ca},a_{so},a_{mg}) &= \Big(a_h - \frac{a_{hco}a_{mg}}{K^m}\Big) = \Big(\gamma_h\rho_h - \frac{\gamma_{mg}\gamma_{hco}\rho_{mg}\rho_{hco}}{K^m}\Big). \end{aligned} \tag{47}$$

Similarly, we introduce activities $a = \gamma\rho$ in the equations (27), (28), and (29) which gives the following relations:

$$C_1 = (\gamma_{hco}\gamma_h)\rho_{hco}\rho_h, \qquad C_2 = \Big(\frac{\gamma_{co}\gamma_h}{\gamma_{hco}}\Big)\frac{\rho_{co}\rho_h}{\rho_{hco}}, \qquad C_w = (\gamma_{oh}\gamma_h)\rho_{oh}\rho_h.$$

Again we use the approximation that we neglect ρ_{co} in the charge balance equation (32) (note that this conservation relation is in terms of the concentrations) yielding

$$C_3(\rho_{ca},\rho_{so},\rho_{mg};\rho_{na},\rho_{cl}) = \rho_{hco} + \rho_{oh} - \rho_h.$$

This gives the relations

$$\begin{aligned} \rho_h &= \frac{1}{2}\Big(-C_3 + \sqrt{C_3^2 + 4(\widetilde{C}_1 + \widetilde{C}_w)}\Big), \qquad \rho_{hco} = \frac{\widetilde{C}_1}{\rho_h}, \\ \rho_{co} &= \frac{\widetilde{C}_2\rho_{hco}}{\rho_h} = \frac{\widetilde{C}_1\widetilde{C}_2}{\rho_h^2}, \qquad \rho_{oh} = \frac{\widetilde{C}_w}{\rho_h}, \end{aligned} \tag{48}$$

where

$$\widetilde{C}_1 = \frac{C_1}{\gamma_{hco}\gamma_h}, \qquad \widetilde{C}_2 = \frac{C_2\gamma_{hco}}{\gamma_{co}\gamma_h}, \qquad \widetilde{C}_w = \frac{C_w}{\gamma_h\gamma_{oh}}, \tag{49}$$

and

$$C_3 = 2(\rho_{ca} + \rho_{mg} - \rho_{so}) + (\rho_{na} - \rho_{cl}).$$

In conclusion,

$$\begin{aligned} \frac{d\rho_{ca}}{dt} &= k_1^c\Big[\mathrm{sgn}^+(\rho_c)F_c^+(\cdot) - F_c^-(\cdot)\Big] + k_1^g\Big[\mathrm{sgn}^+(\rho_g)F_g^+(\cdot) - F_g^-(\cdot)\Big], \\ \frac{d\rho_{so}}{dt} &= k_1^g\Big[\mathrm{sgn}^+(\rho_g)F_g^+(\cdot) - F_g^-(\cdot)\Big], \\ \frac{d\rho_{mg}}{dt} &= k_1^m\Big[\mathrm{sgn}^+(\rho_m)F_m^+(\cdot) - F_m^-(\cdot)\Big], \end{aligned} \tag{50}$$

where

$$\begin{aligned} F_c(\rho_{ca},\rho_{so},\rho_{mg}) &= \Big(\gamma_h\rho_h - \frac{\gamma_{ca}\gamma_{hco}\rho_{ca}\rho_{hco}}{K^c}\Big) = \Big(\gamma_h\rho_h - \frac{\gamma_{ca}C_1\rho_{ca}}{\gamma_h K^c\rho_h}\Big), \\ F_g(\rho_{ca},\rho_{so}) &= \Big(1 - \frac{\gamma_{ca}\gamma_{so}\rho_{ca}\rho_{so}}{K^g}\Big), \\ F_m(\rho_{ca},\rho_{so},\rho_{mg}) &= \Big(\gamma_h\rho_h - \frac{\gamma_{mg}\gamma_{hco}\rho_{mg}\rho_{hco}}{K^m}\Big) = \Big(\gamma_h\rho_h - \frac{\gamma_{mg}C_1\rho_{mg}}{\gamma_h K^m\rho_h}\Big). \end{aligned} \tag{51}$$

In terms of the (x, y, z, u, v, w) variables, the model now takes the form (43) and (44) where (45) is replaced by

$$\begin{aligned} F_c(x,y,z) &= \Big(\gamma_h \rho_h(x,y,z) - \frac{\gamma_{ca} C_1 x}{\gamma_h K^c \rho_h(x,y,z)}\Big), \\ F_g(x,y) &= \Big(1 - \frac{\gamma_{ca}\gamma_{so} xy}{K^g}\Big), \\ F_m(x,y,z) &= \Big(\gamma_h \rho_h(x,y,z) - \frac{\gamma_{mg} C_1 z}{\gamma_h K^m \rho_h(x,y,z)}\Big). \end{aligned} \tag{52}$$

Again, $\rho_h(x, y, z)$ is determined from (48), that is,

$$\begin{gathered} \rho_h(x,y,z) = \frac{1}{2}\Big(-C_3(x,y,z;d) + \sqrt{C_3(x,y,z;d)^2 + 4(\widetilde{C}_1 + \widetilde{C}_w)}\Big), \\ \text{with} \qquad C_3(x,y,z;d) = 2(x - y + z) + d. \end{gathered} \tag{53}$$

3. **Convective and diffusive effects.** Due to dissolution/precipitation of $CaCO_3$, $CaSO_4$, and $MgCO_3$, it might be reasonable to treat the porosity as dependent on the concentration of one or several of the minerals. The following derivation accounts for this possibility. Then, in Section 3.1, we shall assume that the porosity ϕ is constant and focus on that case in the remaining part of the paper. For the moment, we assume more generally that

$$\phi = \phi(\rho_c, \rho_g, \rho_m). \tag{54}$$

Furthermore, we define the porous concentrations of the various components in water as the concentration taken with respect to the volume of the pores. The porous concentrations C_l, C_{na}, C_{cl}, C_{ca}, C_{mg}, and C_{so} are related to the total concentrations by

$$\rho_l = \phi C_l, \ \rho_{na} = \phi C_{na}, \ \rho_{cl} = \phi C_{cl}, \ \rho_{ca} = \phi C_{ca}, \ \rho_{mg} = \phi C_{mg}, \ \rho_{so} = \phi C_{so}. \tag{55}$$

Following Aregba-Driollet et al [1, 2, 3], we argue that since water, Na^+, Cl^-, Ca^{2+}, Mg^{2+}, and SO_4^{2-} flow only through the pores of the calcite specimen, the "interstitial" velocity $\mathbf{v}_l$ associated with the water and $\mathbf{v}_g$ associated with the ions and appearing in (25), have to be defined with respect to the concentrations inside the pores, and differ from the respective seepage velocities $\mathbf{V}_l$ and $\mathbf{V}_g$. The velocities are related by the Dupuit-Forchheimer relations, see [2] and references therein,

$$\mathbf{V}_l = \phi \mathbf{v}_l, \qquad \mathbf{V}_g = \phi \mathbf{v}_g. \tag{56}$$

Consequently, the balance equations (25) can be written in the form

$$\begin{aligned} \partial_t(\phi C_l) + \nabla \cdot (C_l \mathbf{V}_l) &= 0, \\ \partial_t(\phi C_{na}) + \nabla \cdot (C_{na} \mathbf{V}_g) &= 0, \\ \partial_t(\phi C_{cl}) + \nabla \cdot (C_{cl} \mathbf{V}_g) &= 0, \\ \partial_t(\phi C_{ca}) + \nabla \cdot (C_{ca} \mathbf{V}_g) &= \dot{r}_c + \dot{r}_g, \\ \partial_t(\phi C_{so}) + \nabla \cdot (C_{so} \mathbf{V}_g) &= \dot{r}_g, \\ \partial_t(\phi C_{mg}) + \nabla \cdot (C_{mg} \mathbf{V}_g) &= \dot{r}_m, \\ \partial_t \rho_c &= -\dot{r}_c, \\ \partial_t \rho_g &= -\dot{r}_g, \\ \partial_t \rho_m &= -\dot{r}_m. \end{aligned} \tag{57}$$

In order to close the system we must determine the seepage velocities $\mathbf{V}_l$ and $\mathbf{V}_g$. For that purpose we consider the concentration of the water phase (seawater or formation water) C that occupies the pore space as a mixture of water C_l and the various species Na^+, Cl^-, Ca^{2+}, Mg^{2+}, and SO_4^{2-} represented by C_g. In other words,

$$C_g = C_{na} + C_{cl} + C_{ca} + C_{mg} + C_{so}, \qquad C = C_g + C_l. \tag{58}$$

Then, we define the seepage velocity $\mathbf{V}$ associated with C by

$$C\mathbf{V} = C_g\mathbf{V}_g + C_l\mathbf{V}_l. \tag{59}$$

Now we are in a position to rewrite the model in terms of $\mathbf{V}$ and the diffusive velocity $\mathbf{U}_g$ given by

$$\mathbf{U}_g = \mathbf{V}_g - \mathbf{V}. \tag{60}$$

Then the model (57) is given in the form

$$\begin{aligned}
\partial_t(\phi C_l) + \nabla\cdot(C_l\mathbf{V}_l) &= 0,\\
\partial_t(\phi C_{na}) + \nabla\cdot(C_{na}\mathbf{U}_g) &= -\nabla\cdot(C_{na}\mathbf{V}),\\
\partial_t(\phi C_{cl}) + \nabla\cdot(C_{cl}\mathbf{U}_g) &= -\nabla\cdot(C_{cl}\mathbf{V}),\\
\partial_t(\phi C_{ca}) + \nabla\cdot(C_{ca}\mathbf{U}_g) &= (\dot r_c + \dot r_g) - \nabla\cdot(C_{ca}\mathbf{V}),\\
\partial_t(\phi C_{so}) + \nabla\cdot(C_{so}\mathbf{U}_g) &= \dot r_g - \nabla\cdot(C_{so}\mathbf{V}),\\
\partial_t(\phi C_{mg}) + \nabla\cdot(C_{mg}\mathbf{U}_g) &= \dot r_m - \nabla\cdot(C_{mg}\mathbf{V}),\\
\partial_t\rho_c &= -\dot r_c,\\
\partial_t\rho_g &= -\dot r_g,\\
\partial_t\rho_m &= -\dot r_m.
\end{aligned} \tag{61}$$

Furthermore, we can assume that the seepage velocity $\mathbf{V}$ associated with the mixture represented by C, is given by Darcy's law [2, 4, 39]

$$\mathbf{V} = -\frac{\kappa}{\nu}\nabla p, \tag{62}$$

where κ is permeability and ν is viscosity, and p pressure. The diffusive velocity $\mathbf{U}_g$ is expressed by Fick's law by

$$C_\alpha\mathbf{U}_g = -D\nabla C_\alpha, \qquad \alpha = na, cl, ca, so, mg, \qquad D = (\phi D_m + \alpha|\mathbf{V}|)I, \tag{63}$$

where D_m is the effective molecular diffusion coefficient, α is the dispersion length (longitudinal and transversal dispersion lengths are here taken to be equal), and I is the identity tensor. In view of (58) and (63), it follows that

$$C_g\mathbf{U}_g = -D\nabla C_g. \tag{64}$$

Note that we assume that the diffusion coefficient D is the same for all species $\alpha = na, cl, ca, so, mg$. This is a reasonable assumption as long as the concentration

is not too high, see e.g. [8]. Using (62) and (63) in (61) yields

$$\begin{aligned}
\partial_t(\phi C_l) + \nabla\cdot(C_l\mathbf{V}_l) &= 0,\\
\partial_t(\phi C_{na}) - \nabla\cdot(D\nabla C_{na}) &= -\nabla\cdot\Big(C_{na}\mathbf{V}\Big),\\
\partial_t(\phi C_{cl}) - \nabla\cdot(D\nabla C_{cl}) &= -\nabla\cdot\Big(C_{cl}\mathbf{V}\Big),\\
\partial_t(\phi C_{ca}) - \nabla\cdot(D\nabla C_{ca}) &= (\dot r_c + \dot r_g) - \nabla\cdot\Big(C_{ca}\mathbf{V}\Big),\\
\partial_t(\phi C_{so}) - \nabla\cdot(D\nabla C_{so}) &= \dot r_g - \nabla\cdot\Big(C_{so}\mathbf{V}\Big),\\
\partial_t(\phi C_{mg}) - \nabla\cdot(D\nabla C_{mg}) &= \dot r_m - \nabla\cdot\Big(C_{mg}\mathbf{V}\Big),\\
\partial_t\rho_c &= -\dot r_c,\\
\partial_t\rho_g &= -\dot r_g,\\
\partial_t\rho_m &= -\dot r_m,\\
\mathbf{V} &= -\frac{\kappa}{\nu}\nabla p.
\end{aligned} \tag{65}$$

In particular, summing the equations corresponding to C_{na}, C_{cl}, C_{ca}, C_{so}, and C_{mg}, we obtain an equation for C_g in the form

$$\partial_t(\phi C_g) - \nabla\cdot(D\nabla C_g) = (\dot r_c + 2\dot r_g + \dot r_m) + \nabla\cdot\Big(C_g\frac{\kappa}{\nu}\nabla p\Big). \tag{66}$$

In a similar manner, using $C_l\mathbf{V}_l = C_l\mathbf{V} - C_g\mathbf{U}_g$ (obtained from (59), (60), and (58)) in the first equation of (65), the following equation is obtained

$$\partial_t(\phi C_l) + \nabla\cdot(C_l\mathbf{V}) = \nabla\cdot(C_g\mathbf{U}_g), \tag{67}$$

which is equivalent to

$$\partial_t(\phi C_l) - \nabla\cdot(D\nabla[C_l - C]) = \nabla\cdot\Big(C_l\frac{\kappa}{\nu}\nabla p\Big). \tag{68}$$

Summing (68) and (66), we get the following equation for the concentration of the water phase with its different chemical components, represented by $C = C_g + C_l$,

$$\partial_t(\phi C) - \nabla\cdot(D\nabla[C_l - C]) - \nabla\cdot(D\nabla C_g) = (\dot r_c + 2\dot r_g + \dot r_m) + \nabla\cdot\Big(C\frac{\kappa}{\nu}\nabla p\Big), \tag{69}$$

that is,

$$\partial_t(\phi C) - \nabla\cdot\Big(C\frac{\kappa}{\nu}\nabla p\Big) = (\dot r_c + 2\dot r_g + \dot r_m). \tag{70}$$

To sum up, we have a model in the form

$$\begin{aligned}
\partial_t(\phi C) + \nabla\cdot\Big(C\mathbf{V}\Big) &= (\dot r_c + 2\dot r_g + \dot r_m),\\
\partial_t(\phi C_{na}) - \nabla\cdot(D\nabla C_{na}) &= -\nabla\cdot\Big(C_{na}\mathbf{V}\Big),\\
\partial_t(\phi C_{cl}) - \nabla\cdot(D\nabla C_{cl}) &= -\nabla\cdot\Big(C_{cl}\mathbf{V}\Big),\\
\partial_t(\phi C_{ca}) - \nabla\cdot(D\nabla C_{ca}) &= (\dot r_c + \dot r_g) - \nabla\cdot\Big(C_{ca}\mathbf{V}\Big),\\
\partial_t(\phi C_{so}) - \nabla\cdot(D\nabla C_{so}) &= \dot r_g - \nabla\cdot\Big(C_{so}\mathbf{V}\Big),\\
\partial_t(\phi C_{mg}) - \nabla\cdot(D\nabla C_{mg}) &= \dot r_m - \nabla\cdot\Big(C_{mg}\mathbf{V}\Big),\\
\partial_t\rho_c &= -\dot r_c,\\
\partial_t\rho_g &= -\dot r_g,\\
\partial_t\rho_m &= -\dot r_m,\\
\mathbf{V} &= -\frac{\kappa}{\nu}\nabla p,
\end{aligned} \tag{71}$$

where $D = D(\phi)$ as given by (63). The unknowns are C, C_{na}, C_{cl}, C_{ca}, C_{so}, C_{mg}, ρ_c, ρ_g, ρ_m, and p. We have 10 unknowns and 9 equations. We shall assume in the following that the water phase is incompressible, i.e., that C is constant. Another option is to assume that the water mixture is a weakly compressible fluid where we have a constitutive equation for p as a function of C, i.e., $p = p(C)$.

3.1. **Incompressibility.** As a first approach, we follow [2, 3] and assume that the water with its various components is treated as an incompressible fluid, i.e., the concentration C is constant.

$$\begin{aligned}
\partial_t(\phi) - \nabla\cdot\Big(\frac{\kappa}{\nu}\nabla p\Big) &= \frac{1}{C}(\dot r_c + 2\dot r_g + \dot r_m),\\
\partial_t(\phi C_{na}) - \nabla\cdot(D\nabla C_{na}) &= \nabla\cdot\Big(C_{na}\frac{\kappa}{\nu}\nabla p\Big),\\
\partial_t(\phi C_{cl}) - \nabla\cdot(D\nabla C_{cl}) &= \nabla\cdot\Big(C_{cl}\frac{\kappa}{\nu}\nabla p\Big),\\
\partial_t(\phi C_{ca}) - \nabla\cdot(D\nabla C_{ca}) &= (\dot r_c + \dot r_g) + \nabla\cdot\Big(C_{ca}\frac{\kappa}{\nu}\nabla p\Big),\\
\partial_t(\phi C_{so}) - \nabla\cdot(D\nabla C_{so}) &= \dot r_g + \nabla\cdot\Big(C_{so}\frac{\kappa}{\nu}\nabla p\Big),\\
\partial_t(\phi C_{mg}) - \nabla\cdot(D\nabla C_{mg}) &= \dot r_m + \nabla\cdot\Big(C_{mg}\frac{\kappa}{\nu}\nabla p\Big),\\
\partial_t\rho_c &= -\dot r_c,\\
\partial_t\rho_g &= -\dot r_g,\\
\partial_t\rho_m &= -\dot r_m.
\end{aligned} \tag{72}$$

The first equation can be rewritten by making use of the last three equations for the solid components

$$-\Big(\frac{\partial\phi}{\partial\rho_c}\dot r_c + \frac{\partial\phi}{\partial\rho_g}\dot r_g + \frac{\partial\phi}{\partial\rho_m}\dot r_m\Big) - \nabla\cdot\Big(\frac{\kappa}{\nu}\nabla p\Big) = \frac{1}{C}(\dot r_c + 2\dot r_g + \dot r_m),$$

that is,

$$-\nabla\cdot\Big(\frac{\kappa}{\nu}\nabla p\Big) = \frac{1}{C}(\dot r_c + 2\dot r_g + \dot r_m) + \Delta\phi, \tag{73}$$

where $\Delta\phi$ is given by

$$\Delta\phi = \Big(\frac{\partial\phi}{\partial\rho_c}\dot{r}_c + \frac{\partial\phi}{\partial\rho_g}\dot{r}_g + \frac{\partial\phi}{\partial\rho_m}\dot{r}_m\Big). \tag{74}$$

In the remaining part of this paper we shall neglect the change $\Delta\phi$ in the porosity due to chemical precipitation/dissolution of the minerals ρ_c, ρ_g, ρ_m. In other words, we set $\Delta\phi = 0$. The motivation for this is that we first need to understand basic features of this simpler model, and the behavior of this model compared to corresponding experimental results, before we take into account finer mechanisms like dynamic changes in the porosity. Consequently, we shall now deal with the following model:

$$\begin{aligned}
\partial_t(\phi C_{na}) - \nabla\cdot(D\nabla C_{na}) &= \nabla\cdot\Big(C_{na}\frac{\kappa}{\nu}\nabla p\Big),\\
\partial_t(\phi C_{cl}) - \nabla\cdot(D\nabla C_{cl}) &= \nabla\cdot\Big(C_{cl}\frac{\kappa}{\nu}\nabla p\Big),\\
\partial_t(\phi C_{ca}) - \nabla\cdot(D\nabla C_{ca}) &= (\dot{r}_c + \dot{r}_g) + \nabla\cdot\Big(C_{ca}\frac{\kappa}{\nu}\nabla p\Big),\\
\partial_t(\phi C_{so}) - \nabla\cdot(D\nabla C_{so}) &= \dot{r}_g + \nabla\cdot\Big(C_{so}\frac{\kappa}{\nu}\nabla p\Big),\\
\partial_t(\phi C_{mg}) - \nabla\cdot(D\nabla C_{mg}) &= \dot{r}_m + \nabla\cdot\Big(C_{mg}\frac{\kappa}{\nu}\nabla p\Big),\\
\partial_t\rho_c &= -\dot{r}_c,\\
\partial_t\rho_g &= -\dot{r}_g,\\
\partial_t\rho_m &= -\dot{r}_m,\\
-\nabla\cdot\Big(\frac{\kappa}{\nu}\nabla p\Big) &= \frac{1}{C}(\dot{r}_c + 2\dot{r}_g + \dot{r}_m).
\end{aligned} \tag{75}$$

The unknown variables we solve for are C_{na}, C_{cl}, C_{ca}, C_{so}, C_{mg}, ρ_c, ρ_g, ρ_m, and pressure p.

Remark 5. For a more complete model it would be reasonable to let the permeability κ also depend on the concentration of the solid components, i.e., $\kappa = \kappa(\rho_c, \rho_g, \rho_m)$ similar to the porosity. However, consistent with the above assumption about constant porosity, it is at the current stage natural to assume that the permeability is also constant.

Noting that the molar density for water is $C_l = 5.56\times10^4$ mol/m^3 = 55.6mol/liter [43], the molar concentrations associated with the reaction terms $\dot{r}_c$, $\dot{r}_g$, and $\dot{r}_m$ describing precipitation/dissolution of $CaCO_3$, $CaSO_4$, and $MgCO_3$, is expected to be considerable smaller than C. A natural consequence is then that the right-hand side term in the last equation of (75) can be neglected. This approximation is applied in the following, implying that the pressure gradient is constant and must be determined from, for example, known injection rate.

3.2. **Scaled version of the model.** In the following we shall restrict ourselves to a one-dimensional version of the model (75). First, we introduce the variables

$$\begin{aligned}
&b = \phi C_{na}, \quad c = \phi C_{cl}, \quad x = \phi C_{ca}, \quad y = \phi C_{so}, \quad z = \phi C_{mg},\\
&u = \rho_c, \quad v = \rho_g, \quad w = \rho_m,
\end{aligned} \tag{76}$$

consistent with (42). Let τ be the time scale of the problem. Then, an appropriate space scale could be given by the diffusive typical length

$$L = \sqrt{\overline{D}_m \tau}, \tag{77}$$

where $\overline{D}_m$ is a reference diffusion coefficient. We then define dimensionless space s and time t variables as follows

$$s' = \frac{s}{\sqrt{\overline{D}_m \tau}}, \qquad t' = \frac{t}{\tau}, \tag{78}$$

and dimensionless coefficients

$$D'_m = \frac{D_m}{\overline{D}_m}, \qquad \kappa' = \frac{\kappa}{\overline{\kappa}}, \qquad p' = \frac{p}{\overline{p}}, \tag{79}$$

where $\overline{p}$ is a reference pressure, $\overline{\kappa}$ is reference permeability, and $\overline{D}_m$ reference diffusion coefficient. Using that $D = \phi D_m + \frac{\alpha\kappa}{\nu}|\partial_s p|$ and that ϕ is constant, we get the following form of the model (75)

$$\begin{aligned}
\partial_{t'}(b) - \partial_{s'}(D'_m \partial_{s'} b) &= \varepsilon \partial_{s'}\Big(b\frac{\kappa'}{\phi}\partial_{s'}p' + \mu\frac{\kappa'}{\phi}|\partial_{s'}p'|\partial_{s'}b\Big),\\
\partial_{t'}(c) - \partial_{s'}(D'_m \partial_{s'} c) &= \varepsilon \partial_{s'}\Big(c\frac{\kappa'}{\phi}\partial_{s'}p' + \mu\frac{\kappa'}{\phi}|\partial_{s'}p'|\partial_{s'}c\Big),\\
\partial_{t'}(x) - \partial_{s'}(D'_m \partial_{s'} x) &= \tau(\dot r_c + \dot r_g) + \varepsilon \partial_{s'}\Big(x\frac{\kappa'}{\phi}\partial_{s'}p' + \mu\frac{\kappa'}{\phi}|\partial_{s'}p'|\partial_{s'}x\Big),\\
\partial_{t'}(y) - \partial_{s'}(D'_m \partial_{s'} y) &= \tau \dot r_g + \varepsilon \partial_{s'}\Big(y\frac{\kappa'}{\phi}\partial_{s'}p' + \mu\frac{\kappa'}{\phi}|\partial_{s'}p'|\partial_{s'}y\Big),\\
\partial_{t'}(z) - \partial_{s'}(D'_m \partial_{s'} z) &= \tau \dot r_m + \varepsilon \partial_{s'}\Big(z\frac{\kappa'}{\phi}\partial_{s'}p' + \mu\frac{\kappa'}{\phi}|\partial_{s'}p'|\partial_{s'}y\Big),\\
\partial_{t'} u &= -\tau \dot r_c,\\
\partial_{t'} v &= -\tau \dot r_g,\\
\partial_{t'} w &= -\tau \dot r_m,\\
-\varepsilon \partial_{s'}\Big(\kappa' \partial_{s'} p'\Big) &= \frac{\tau}{C}(\dot r_c + \dot r_g + \dot r_m),
\end{aligned} \tag{80}$$

with

$$\varepsilon = \frac{\overline{\kappa}\,\overline{p}}{\nu \overline{D}_m}, \qquad \mu = \frac{\alpha}{\sqrt{\overline{D}_m \tau}}. \tag{81}$$

As indicated above, we shall neglect the precipitation/dissolution effects on the pressure equation, i.e., the right hand side of the last equation of (80) is set to zero. This implies that

$$J := -\varepsilon \kappa' \partial_{s'} p' = \text{Constant},$$

and will be determined from known information about the injection rate. We define

$$V(t) := \frac{J(t)}{\phi}, \tag{82}$$

where the t-dependency account for possible variations in the injection rate as time is running. We may, for the sake of simplicity, set the dispersion length to zero

$\alpha = 0$, which implies that $\mu = 0$. Consequently, we have the model (where we have skipped the 'prime' index)

$$\begin{aligned}
\partial_t(b) + \partial_s(bV(t)) &= \partial_s(D_m\partial_s b),\\
\partial_t(c) + \partial_s(cV(t)) &= \partial_s(D_m\partial_s c),\\
\partial_t(x) + \partial_s(xV(t)) &= \partial_s(D_m\partial_s x) + \tau(\dot{r}_c + \dot{r}_g),\\
\partial_t(y) + \partial_s(yV(t)) &= \partial_s(D_m\partial_s y) + \tau\dot{r}_g,\\
\partial_t(z) + \partial_s(zV(t)) &= \partial_s(D_m\partial_s z) + \tau\dot{r}_m,\\
\partial_t u &= -\tau\dot{r}_c,\\
\partial_t v &= -\tau\dot{r}_g,\\
\partial_t w &= -\tau\dot{r}_m.
\end{aligned} \tag{83}$$

The model must be equipped with appropriate initial conditions

$$\begin{aligned}
&b|_{t=0} = b_0(s), \quad c|_{t=0} = c_0(s), \quad x|_{t=0} = x_0(s), \quad y|_{t=0} = y_0(s), \quad z|_{t=0} = z_0(s),\\
&u|_{t=0} = u_0(s), \quad v|_{t=0} = v_0(s), \quad w|_{t=0} = w_0(s),
\end{aligned} \tag{84}$$

and Dirichlet boundary conditions at the left end of the domain

$$b|_{s=0} = b_L, \quad c|_{s=0} = c_L, \quad x|_{s=0} = x_L, \quad y|_{s=0} = y_L, \quad z|_{s=0} = z_L, \tag{85}$$

where the brine with a known concentration of the different ions is injected into the core plug. At the right end, where the brine leaves the core, we use extrapolation. This model corresponds to (7) under the assumption of constant porosity ϕ and constant fluid velocity (in space). In the next section we describe a discretization strategy for solving the model (83)–(85). We note that the assumption about constant porosity removes a potential strong nonlinear coupling between the various equations. Instead all the coupling goes through the source terms. This class of convection-diffusion-reaction models is often referred to as *weakly coupled* [27]. This model also represents an extended version of the model studied in [8] and is similar to the model studied in [20]. A natural solution strategy for this type of problem is an operator-splitting approach as described in the next section.

4. **Discrete approximations.**

4.1. **Numerical discretization.**

Let us introduce $\mathbf{U} = (u, v, w)^T$ and $\mathbf{C} = (b, c, x, y, z)^T$. We assume that we have approximate solutions $(\mathbf{U}^n(\cdot), \mathbf{C}^n(\cdot)) \approx (\mathbf{U}(\cdot, t^n), \mathbf{C}(\cdot, t^n))$. Now, we want to calculate an approximation at the next time level $(\mathbf{U}^{n+1}(\cdot), \mathbf{C}^{n+1}(\cdot)) \approx (\mathbf{U}(\cdot, t^{n+1}), \mathbf{C}(\cdot, t^{n+1}))$ by using a two-step operator splitting approach [31, 20].

Step 1: Chemical reactions. Let S_t be the operator associated with the solution of the following system of ODEs:

$$\begin{aligned}
\frac{db}{dt} =& 0,\\
\frac{dc}{dt} =& 0,\\
\frac{dx}{dt} =& A_1^c\Big[\mathrm{sgn}^+(u)F_c^+(x,y,z) - F_c^-(x,y,z)\Big]\\
&+ A_1^g\Big[\mathrm{sgn}^+(v)F_g^+(x,y,z) - F_g^-(x,y,z)\Big],\\
\frac{dy}{dt} =& A_1^g\Big[\mathrm{sgn}^+(v)F_g^+(x,y,z) - F_g^-(x,y,z)\Big],\\
\frac{dz}{dt} =& A_1^m\Big[\mathrm{sgn}^+(w)F_m^+(x,y,z) - F_m^-(x,y,z)\Big],\\
\frac{du}{dt} =& -A_1^c\Big[\mathrm{sgn}^+(u)F_c^+(x,y,z) - F_c^-(x,y,z)\Big],\\
\frac{dv}{dt} =& -A_1^g\Big[\mathrm{sgn}^+(v)F_g^+(x,y,z) - F_g^-(x,y,z)\Big],\\
\frac{dw}{dt} =& -A_1^m\Big[\mathrm{sgn}^+(w)F_m^+(x,y,z) - F_m^-(x,y,z)\Big],
\end{aligned} \tag{86}$$

where $A_1^I = \tau k_1^I$, for $I = c, g, m$. Here F_I is given by (52) and (53). That is, we solve a model of the following form

$$\begin{aligned}
\frac{d\mathbf{C}}{dt} = \mathbf{F}(\mathbf{U},\mathbf{C}), \qquad \frac{d\mathbf{U}}{dt} = \mathbf{G}(\mathbf{U},\mathbf{C}), \qquad t\in(0,\Delta t],\\
\mathbf{C}(\cdot,0) = \mathbf{C}^n(\cdot), \qquad \mathbf{U}(\cdot,0) = \mathbf{U}^n(\cdot).
\end{aligned} \tag{87}$$

Note that this system corresponds to solving (43) and (44) with F_I given by (52) and (53). From this we obtain intermediate approximations $(\mathbf{C}^{n+1/2}, \mathbf{U}^{n+1/2}) = S_{\Delta t}(\mathbf{C}^n, \mathbf{U}^n)$.

Remark 6. The stiff ODE system given by (86) is in this work solved by using the Matlab function ode23.

Step 2: Convection and diffusion. Let D_t be the operator associated with the solution of the following system of parabolic PDEs:

$$\begin{aligned}
\partial_t(b) + \partial_s(bV(t)) &= \partial_s(D_m\partial_s b),\\
\partial_t(c) + \partial_s(cV(t)) &= \partial_s(D_m\partial_s c),\\
\partial_t(x) + \partial_s(xV(t)) &= \partial_s(D_m\partial_s x),\\
\partial_t(y) + \partial_s(yV(t)) &= \partial_s(D_m\partial_s y),\\
\partial_t(z) + \partial_s(zV(t)) &= \partial_s(D_m\partial_s z),\\
\partial_t u &= 0,\\
\partial_t v &= 0,\\
\partial_t w &= 0.
\end{aligned} \tag{88}$$

That is, the model we solve is in the form

$$\begin{aligned}
\partial_t(\mathbf{C}) + \partial_s(\mathbf{C}V(t)) = \partial_s(D_m\partial_s\mathbf{C}), \qquad \mathbf{U}(\cdot,t) = \mathbf{U}^{n+1/2}(\cdot), \qquad t\in(0,\Delta t],\\
\mathbf{C}(\cdot,0) = \mathbf{C}^{n+1/2}(\cdot).
\end{aligned} \tag{89}$$

From this we find $(\mathbf{C}^{n+1}, \mathbf{U}^{n+1}) = D_{\Delta t}(\mathbf{C}^{n+1/2}, \mathbf{U}^{n+1/2})$.

Remark 7. Concerning the discretization of the convection-diffusion model (88), several options are possible. First, we could use an explicit time discretization, an implicit treatment, or a convex combination of explicit and implicit similar to Aregba-Driollet et al [1, 3]. Another option could be to follow Nie et al and use an integration factor approach where the linear diffusion is treated exactly [38, 13]. Note however that this requires that the diffusion coefficient is a constant, i.e., ϕ is taken to be constant. This method was also presented only for a diffusion-reaction system. Hence, for the sake of simplicity, we currently use an explicit central based discretization of the diffusion terms together with the second order relaxed-scheme fluxes, similar to what we used in [49], for the discretization of the convective terms.

Remark 8. In the following we shall use the Strang type of splitting [20, 48]:

$$(\mathbf{C}^{n+1}, \mathbf{U}^{n+1}) = [D_{\Delta t/2} S_{\Delta t} D_{\Delta t/2}](\mathbf{C}^{n}, \mathbf{U}^{n}). \tag{90}$$

We do no attempt to optimize the numerical method we apply. Main focus, at this stage, is on basic properties of the model itself in terms of its capability to capture important coupled flow and precipitation/dissolution mechanisms as observed through the laboratory experiments.

5. Numerical investigations.

The purpose of this section is twofold. Firstly, we want to perform an evaluation of the model (83)–(85) by comparison with some recent laboratory experiments where chalk core plugs are flooded with a brine which contains only $MgCl_2$. Such type of experiments, with many different brines, have been explored extensively during the last ten years, see for example [21, 32, 29] and references therein. The experiments we compare the model with also involve measurements of the creep behavior when the core is subject to stress. Currently, such effects are not included in the model. Focus is on the interaction between transport effects and chemical reactions, as observed by changes in ion concentrations at the outlet. Secondly, we seek further insight into characteristic features of the model by varying the injection rate and thereby causing a change in the balance between flow and dissolution/precipitation. Finally, we also explore the behavior predicted by the model when the length of the core is increased.

5.1. Experimental setup.

A brief description of the experimental setup for the simplified system follows, we refer to [33] for more details. The purpose of these experiments is not to simulate any water injection of North Sea chalk reservoirs at in-situ stress conditions, however, rather to select a repeatable type of tests in order to gain further in depth understanding behind the mechanisms causing the water weakening of chalks. Hydrostatic- and creep tests with continuous flooding of various fluids, at an injection rate equal to approximately 1 pore volume per day (1 PV/D), were performed in a standard hydraulically operated triaxial cell equipped with a heat regulating system. During the experiments the temperature was kept constant; 130°C.

Prior to the mechanical testing each chalk core was saturated with distilled water and thereafter the core was mounted in the triaxial cell; the confining -and pore pressure were simultaneously increased to an effective stress equal to 0.5 MPa (confining pressure 1.2 MPa and pore pressure 0.7 MPa) while cleaning the cores by flooding a minimum of 2 pore volumes distilled water. After cleaning, flooding of

the respective fluid was started and the triaxial cell was heated to chosen test temperature, 130°C. Then the sample was left over night to equilibrate at a constant flooding rate of 1 PV/D. The following day the sample was isotropically loaded beyond yield, which are the point where the stress-strain curve departs from the linear trend, and thereafter left to creep at an effective stress level of 10.5 MPa. Flooding effluent was continuously fractioned during the entire test period and analyzed by use of an Ion Chromatograph.

5.2. **Input data for the model.** We consider a core of length $L = 0.07$ m. We use the reference time $\tau = 1$ day $= 24 \cdot 3600$ sec. In view of (77), this corresponds to a reference molecular diffusion coefficient $\overline{D}_m = L^2/\tau = 5.6713 \cdot 10^{-8}$ m^2/s. We want to determine $J = -\varepsilon\kappa\partial_s p$ (constant) from the known injection rate $Q = q$ PV/day, where q is a dimensionless quantity, typically around 1 and PV represents pore volume. In particular,

$$Q = q\frac{\phi AL}{\tau}, \tag{91}$$

where A is the area of an intersection of the core, L is length of the core, and τ is the reference time. Clearly, in accordance with Darcy's law, we have

$$Q = -\frac{\kappa\overline{\kappa}A}{\nu}\Big(\frac{\Delta P}{L}\Big). \tag{92}$$

Combining (91) and (92) gives the relation

$$q\frac{\phi L}{\tau} = -\frac{\kappa\overline{\kappa}}{\nu}\Big(\frac{\Delta P}{L}\Big), \qquad \text{or} \qquad \frac{\Delta P}{\overline{p}} = -q\frac{\phi L^2\nu}{\tau\kappa\overline{\kappa}\,\overline{p}}.$$

In light of (81) we note that

$$\varepsilon\kappa\partial_x p = \varepsilon\kappa\frac{\Delta P}{\overline{p}} = -q\frac{\phi L^2}{\overline{D}_m\tau} = -q\frac{\phi\overline{D}_m\tau}{\overline{D}_m\tau} = -q\phi,$$

by using that $\overline{D}_m = L^2/\tau$. In other words,

$$J = -\varepsilon\kappa\partial_s p = q\phi.$$

Thus, in view of (82), we conclude that $V(t) = q$ in (83).

Activity coefficients. We consider the simplified system composed of water, Cl^-, and Mg^{2+} ions. The values for chemical activity coefficients we use, relevant for the simplified flow system considered at temperature $T = 130$°C, are calculated as follows. First, according to the Debuye-Hückel equation, see for example [41, 30, 10], the activity γ_i is given by

$$-\log_{10}(\gamma_i) = \frac{AZ_i^2\sqrt{I_0}}{1 + a_i^0 B\sqrt{I_o}}, \tag{93}$$

where the index i refers to the different species involved. Moreover, Z_i refers to the ionic charges, $A(T)$ and $B(T)$ are temperature dependent given functions, and I_0 refers to the ionic strength defined by

$$I_0 = \frac{1}{2}\sum_i \rho_i Z_i^2. \tag{94}$$

The following values, taken from [10, 26], are used for the constants a_i^0:

$$\begin{aligned} &a_h^0 = 9, \quad a_{oh}^0 = 3.5, \quad a_{ca}^0 = 6, \quad a_{hco}^0 = 4, \\ &a_{na}^0 = 4, \quad a_{cl}^0 = 3, \quad a_{mg}^0 = 8, \quad a_{so}^0 = 4, \quad a_{co} = 4.5. \end{aligned} \tag{95}$$

Moreover, we shall use the following values for $A(T)$ and $B(T)$ taken from [10, 26]:

$$A(T = 130) = 0.6623, \qquad B(T = 130) = 0.3487. \tag{96}$$

Moreover, the following solubility products are used:

	T=25	T=70	T=90	T=130
K^c	$10^{+1.86}$	$10^{+1.21}$	$10^{+0.92}$	$10^{+0.35}$
K^g	$10^{-4.3}$	$10^{-4.87}$	$10^{-5.21}$	$10^{-5.94}$
K^m	$10^{+2.3}$	$10^{+1.24}$	$10^{+0.79}$	$10^{-0.01}$
K	$10^{-7.87}$	$10^{-8.05}$	$10^{-8.33}$	$10^{-9.01}$
C_w	$10^{-14.05}$	$10^{-12.72}$	$10^{-12.47}$	$10^{-12.26}$
C_2	$10^{-10.32}$	$10^{-10.09}$	$10^{-10.08}$	$10^{-10.15}$

K^c, K^g, K^m refer to (15)–(18), K refer to (27), C_2 refer to (28), and C_w to (29). In order to calculate C_1 in (27), we have used the given K value from the above table and the CO_2 partial pressure P_{CO_2} constant is set to $P_{CO_2} = 10^{-3.5}$, see also [33]. All these constants have been taken from the EQAlt-simulator [10, 26].

5.3. **Study of a simplified laboratory core plug experiment.**

Core properties.

- Length $L = 0.07\,\mathrm{m}$
- Porosity $\phi = 0.48$
- Volume of core $V_c = 75\,\mathrm{ml}$
- Volume of matrix $V_m = 36\,\mathrm{ml}$
- Mass of rock $M_c = 100\,\mathrm{g}$

In view of the fact that the molecular weight of $CaCO_3$ is 100g/mol, it follows that the solid part of the core corresponds to 1 mol $CaCO_3$. Consequently, the molar density is $\rho_c = 1/V_m\,\mathrm{mol/liter} \approx 28\,\mathrm{mol/liter}$.

Some parameters. In this section, parameters for convection, diffusion, and reactions are chosen as follows:

$$k_1^c = 60, \qquad k_1^g = k_1^c, \quad \text{and} \quad k_1^m = 0.08 k_1^c \ \ (\text{in terms of } (\mathrm{mol/liter})\,\mathrm{sec}^{-1}) \tag{97}$$

$$q = 1.3, \qquad D_m = 6 \cdot 10^{-8}\,\mathrm{m}^2/\mathrm{s}. \tag{98}$$

The choice of q and D_m are motivated as follows: From the experimental setup, the injection rate should be approximately 1 PV/day. We have set $q = 1.3$, and the choice of the molecular diffusion coefficient has then be made such that the concentration profile for Cl^-, given by ρ_{cl}, as a function of time measured at the outlet, fits reasonable well with the experimental behavior, see Figs. 1 and 2. The underlying assumption here, and also used in the model, is that Cl^- to a minor extent is active in the chemical reactions but are transported through the core as a result of the convective and diffusive forces only.

Case I: $0.109\,\textbf{mol MgCl}_2$**.**

Initial and boundary data. As initial data for this first case we have a core composed of the mineral $CaCO_3$. As described above, the following densities (mol/liter) are given initially for the minerals associated with the core

$$\rho_{c,0} = 28, \qquad \rho_{g,0} = 0, \qquad \rho_{m,0} = 0.$$

Moreover, it is assumed that the core is initially filled with pure water, in other words, all ion concentrations are set to zero inside the core. As far as boundary conditions are concerned, we shall consider a case where a water mixture with $0.109\,\text{mol}\ MgCl_2$ is injected at the left inlet with a constant rate. In particular, the concentration (mol/liter) of Mg^{2+} and Cl^- at the left inlet is set to

$$\rho_{cl,L} = 0.218, \qquad \rho_{ca,L} = 0, \qquad \rho_{mg,L} = 0.109.$$

We use the concentration of the injected mixture of $MgCl_2$ given by 0.109 mol to calculate the ionic strength I_0 given by (94)

$$I_0^{(1)} = 0.3270. \tag{99}$$

This, in turn, allows us to calculate the various activity coefficients from (93) by using (95) and (96). In particular, the following values are obtained:

$$\begin{array}{lllll} \gamma_{ca} = 0.204 & \gamma_{so} = 0.144 & \gamma_{mg} = 0.261 & \gamma_{na} = 0.616 & \gamma_{cl} = 0.580 \\ \gamma_{h} = 0.732 & \gamma_{oh} = 0.598 & \gamma_{co} = 0.159 & \gamma_{hco} = 0.616. & \end{array} \tag{100}$$

Verification of convergence properties. We check that the obtained approximations are not sensitive relative the grid that is used. A reasonable choice of discretization parameters turns out to be a grid of $N = 60$ cells and a time splitting step corresponding to $\Delta t = 1\,\text{hour}$, at least for the reaction rates we have used. When reaction rates becomes large, the chemical reactions take place on a faster time scale, and the number of time splitting steps should be increased in order to capture accurately the balance between flow and dissolution/precipitation. We also mention that, given the initial ion concentrations inside the core, we find updated concentrations such that the system is in thermodynamical equilibrium before we start the flooding.

Comparison with experimental data. From Fig. 1, the following observations are made:

- The experimental concentration profiles reflect that there is a loss of Mg^{2+} ions inside the core and a production of Ca^{2+} ions. After some time (approximately 8000 minutes) a steady state is reached. Clearly, the results produced by the proposed model fit well with the experimental results, and indicate that the ion concentrations of Mg^{2+} and Ca^{2+} can be understood as a result of an interplay betweeen (i) convection and diffusion; (ii) dissolution of $CaCO_3$ and precipitation of $MgCO_3$.
- The measured concentration profiles indicate that the sum of the concentration of Mg^{2+} and Ca^{2+} remains constant and close to the concentration of Mg^{2+} in the injected water mixture, that is, 0.109 mol/liter. The model explains this behavior in terms of dissolution and precipitation.
- The experimental behavior of Ca^{2+} and Mg^{2+} during the first time period (up to approximately 2000 minutes), is somewhat unclear. Clearly, the rapid increase in the ion concentration of Ca^{2+} before it slowly decreases towards a steady state, is not taken into account by the model.

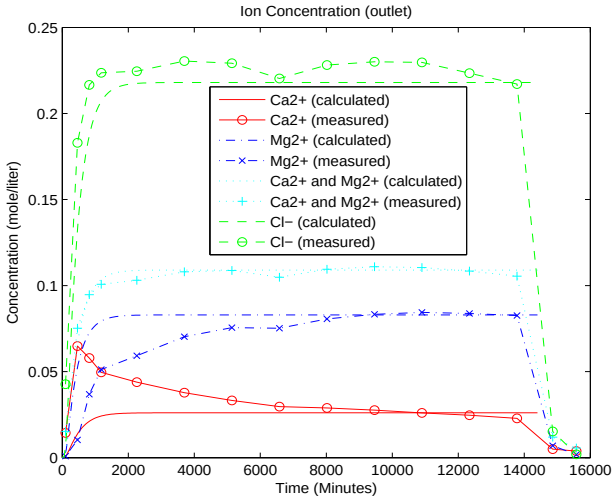

FIGURE 1. **Case I**. Concentrations at outlet for various ions, Ca^{2+}, Mg^{2+}, and Cl^{-}. Comparison between experimental results and calculated solutions of the model for a brine with 0.109 mol $MgCl_2$.

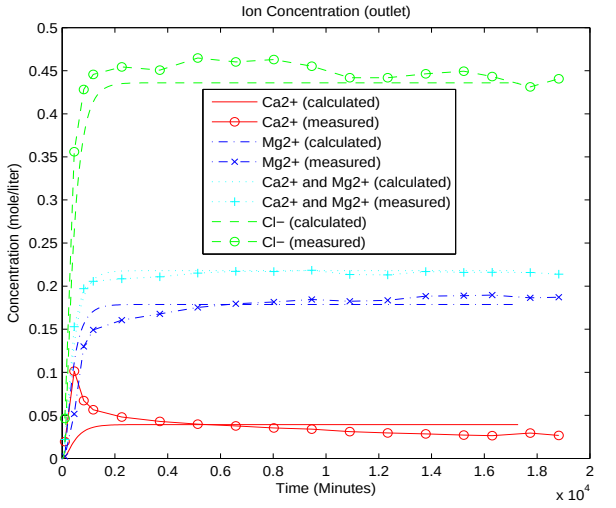

FIGURE 2. **Case II**. Concentrations at outlet for various ions, Ca^{2+}, Mg^{2+}, and Cl^{-}. Comparison between experimental results and calculated solutions of the model for a brine of 0.218 mol $MgCl_2$.

Case II: 0.218 **mol $MgCl_2$.**

Initial and boundary data. This example is very similar to the first where we now have doubled the concentration of $MgCl_2$. That is, a water mixture with 0.218 mol

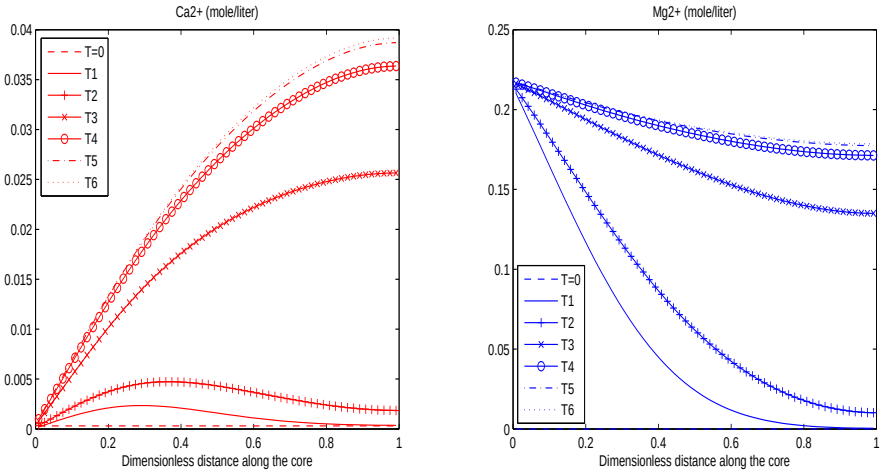

FIGURE 3. **Case II**. Concentration of Ca^{2+} (left) and Mg^{2+} (right) along the core at initial time $T_0 = 0$ and at times $T_1 = 1$, $T_2 = 2$, $T_3 = 10$, $T_4 = 20$, $T_5 = 30$, and $T_6 = 40$ hours. Convergence to steady state profiles is demonstrated.

$MgCl_2$ is injected at the left inlet with the same constant rate. Hence, the concentration (mol/liter) of Mg^{2+} and Cl^- at the left inlet is set to

$$\rho_{cl,L} = 0.436, \qquad \rho_{ca,L} = 0, \qquad \rho_{mg,L} = 0.218.$$

We use the concentration of the injected mixture of $MgCl_2$ given by 0.218 mol to calculate the ionic strength I_0 given by (94)

$$I_0^{(2)} = 0.6540. \tag{101}$$

This, in turn, allows us to calculate the various activity coefficients from (93) by using (95) and (96). In particular, the following values are obtained:

$$\begin{array}{lllll} \gamma_{ca} = 0.160 & \gamma_{so} = 0.099 & \gamma_{mg} = 0.220 & \gamma_{na} = 0.560 & \gamma_{cl} = 0.513 \\ \gamma_{h} = 0.706 & \gamma_{oh} = 0.538 & \gamma_{co} = 0.114 & \gamma_{hco} = 0.560. & \end{array} \tag{102}$$

Again we use the parameters given by (97) and (98) in the model. The resulting concentration profiles, both experimental and computed, are shown in Fig 2. The steady state levels of the ion concentrations measured at the outlet fit well with the computed concentrations. Clearly, the model seems to capture some of essential flow/chemical reaction mechanisms for this simplified water-rock system.

Finally, we want to study the behavior predicted by the model concerning the distribution of the various ion concentrations along the core for different times for the case with 0.218 mol $MgCl_2$. This also gives a visualization of the precipitation/dissolution of the minerals inside the core plug. First, in Fig. 3 the concentrations of Ca^{2+} (left figure) and Mg^{2+} (right figure) at different times are presented. The left figure clearly demonstrates how the injection of the $MgCl_2$ brine (without Ca^{2+}) leads to a low concentration close to the left inlet. However, there is a steady dissolution of $CaCO_3$ that produces Ca^{2+} ions inside the core. As time becomes large enough, a steady state concentration profile is reached. This profile marks a situation where a perfect balance between convection, diffusion, and reaction has

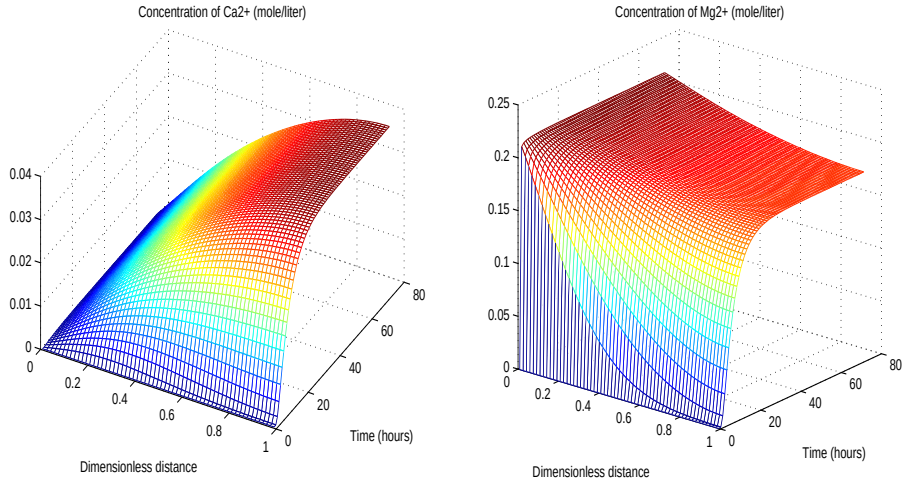

FIGURE 4. **Case II**. Concentration of Ca^{2+} (left) and Mg^{2+} (right) during the first 3 days of flooding.

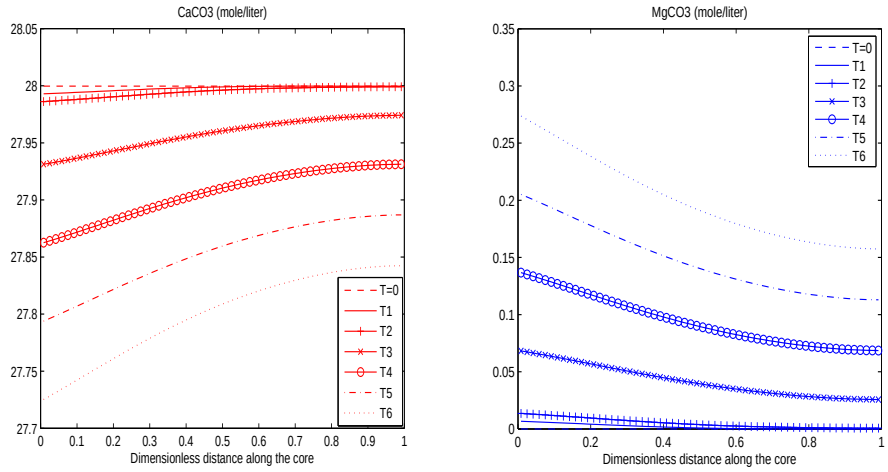

FIGURE 5. **Case II**. Concentration of $CaCO_3$ (left) and $MgCO_3$ (right) along the core at initial time $T_0 = 0$ and at times $T_1 = 1$, $T_2 = 2$, $T_3 = 10$, $T_4 = 20$, $T_5 = 30$, and $T_6 = 40$ hours. Dissolution of $CaCO_3$ and precipitation of $MgCO_3$.

been reached. In a similar manner, the figure for Mg^{2+} shows that there is a steady precipitation of $MgCO_3$ that consumes Mg^{2+} ions inside the core such that the concentration of Mg^{2+} in the injected water cannot be reached throughout the core. A visualization of the change in space and time is also shown in Fig. 4.

The corresponding concentration profiles for the minerals considered at the same times, are shown in Fig. 5. The left figure clearly demonstrates the steady dissolution of $CaCO_3$ taking place inside the core as time is running. Similarly, the right

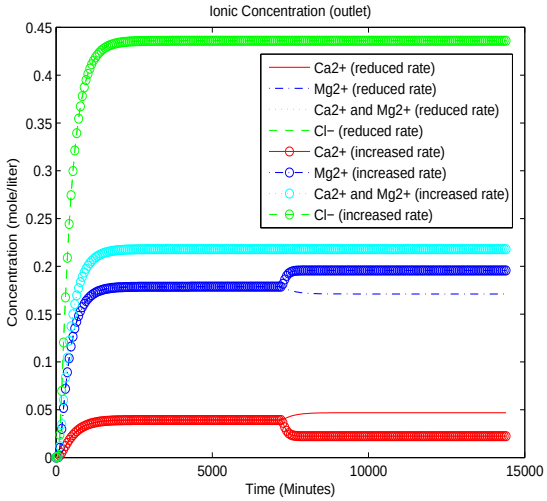

FIGURE 6. **Case II**. Concentrations at outlet for various ions, Ca^{2+}, Mg^{2+}, and Cl^{-} where we increase or decrease the injection rate q after $T = 5$ days.

figure shows the corresponding precipitation of $MgCO_3$. Note that these dissolution/precipitation processes will continue as long as there is still more $CaCO_3$ left to be dissolved. Ultimately, it should lead to changes in the pore structure that can be observed experimentally.

Reduction of injection rate. We now want to explore how the ion concentration profiles at the outlet depends on the injection rate. We consider the example with injection of a water mixed with 0.218 mol $MgCl_2$. We run the flooding for 10 days. For the first 5 days, the injection rate is q=1.3 as before. Then we reduce it to $q/4$. Afterwards, we run a similar example, however, now the rate is increased to $4q$ after 5 days. The results are shown in Fig. 6. Clearly, when the injection rate is increased after 5 days, the dissolution of $CaCO_3$ goes down. In other words, the production of Ca^{2+} decreases and the concentration of Mg^{2+} shows a corresponding increase reflecting that the precipitation of $MgCO_3$ also decreases. Similarly, when the injection rate is reduced after 5 days, this will imply a stronger dissolution of $CaCO_3$ (increase of Ca^{2+}) and stronger precipitation of $MgCO_3$ (decrease of Mg^{2+}). However, the changes in these ion concentrations are relatively small since the molecular diffusion remains the same and now represents a relatively strong part of the transport effect. In this sense, we may say that the dissolution/precipitation processes are dictated by convection and diffusion.

5.4. **Uscaling to a larger core plug.** Finally, we would like to employ the model to predict the behavior for an upscaled problem. That is, we consider a core which is ten times the length of the core used in the experiments and used for the above simulations. Otherwise, parameters are set as before. In particular, the injection rate should now be one tenth of the injection rate used above. That is,

- $L = 0.7$ m
- $q = 0.13$.

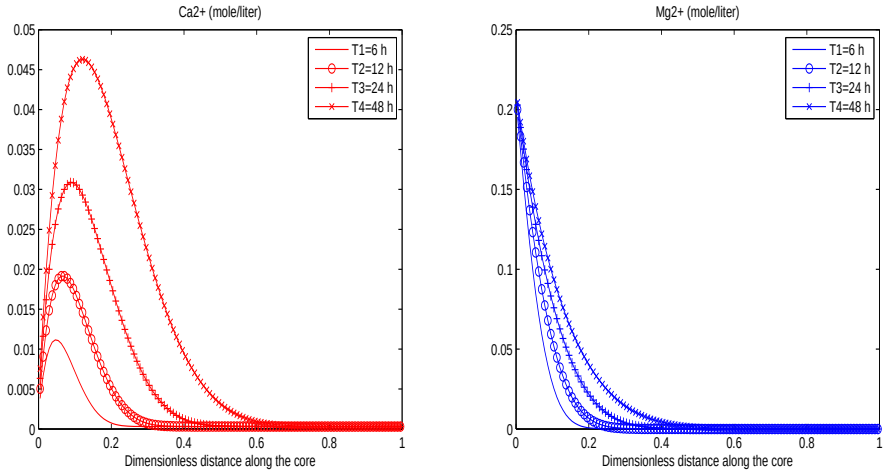

FIGURE 7. **Case II**. In situ concentrations for the ions Ca^{2+} and Mg^{2+} after $T_1 = 6$, $T_2 = 12$, $T_3 = 24$, and $T_4 = 48$ hours with a long core, $L = 0.7$ m.

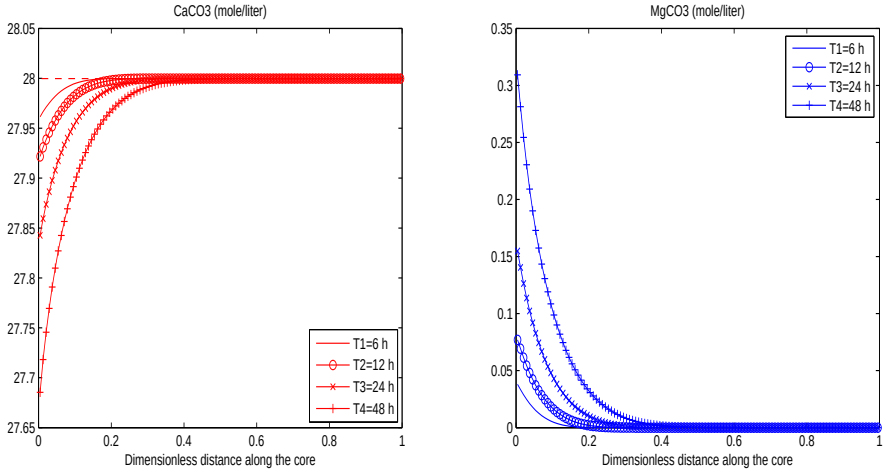

FIGURE 8. **Case II**. In situ concentrations for the minerals $CaCO_3$ and $MgCO_3$ after $T_1 = 6$, $T_2 = 12$, $T_3 = 24$, and $T_4 = 48$ hours with a long core, $L = 0.7$ m.

We have used a grid of 120 cells and consider the situation after $T = 2$ days. We apply 960 time splitting steps, i.e., $\Delta t = 3$ minutes. The various ion concentrations are shown in Fig. 7 and the corresponding concentrations for the minerals are shown in Fig. 8. A characteristic dissolution/precipitation front is seen in Fig. 8 that moves from left to right. A corresponding "pulse"-like concentration for Ca^{2+}, see Fig. 7, is generated that reflects the production of these ions due to dissolution of $CaCO_3$.

Further investigations of the speed of the dissolution/precipitation front, as well as its sensitivity for various parameters, are certainly of interest and will be addressed in the forthcoming time. The growth rate of the "thickness" of the dissolved layer of $CaCO_3$ (see Fig. 8), and knowledge about different parameters that affect this rate, also becomes important when we want to extract information relevant for chalk weakening effects on the reservoir scale.

Acknowledgments. The authors are grateful for insightful comments from Dr. O. Vikane (IRIS) and Dr. L.M. Cathles (Cornell University, USA). The authors also would like to thank the referees for their valuable comments and suggestions.

REFERENCES

[1] D. Aregba-Driollet, F. Diele and R. Natalini, *A mathematical model for the sulphur dioxide aggression to calcium carbonate stones: Numerical approximation and asymptotic analysis*, SIAM J. Appl. Math., **64** (2004), 1636–1667.

[2] G. Ali, V. Furuholt, R. Natalini and I. Torcicollo, *A mathematical model of sulphite chemical aggression of limestones with high permeability. Part I. Modeling and qualitative analysis*, Transport Porous Med, **69** (2007), 109–122.

[3] G. Ali, V. Furuholt, R. Natalini and I. Torcicollo, *A mathematical model of sulphite chemical aggression of limestones with high permeability. Part II. Numerical approximation*, Transport Porous Med, **69** (2007), 175–188.

[4] G. I. Barenblatt, V. M. Entov and V. M. Ryzhik, "Theory of Fluid Flows Through Natural Rocks," Kluwer Academic Publisher, 1990.

[5] G. I. Barenblatt, M. Bertsch and C. Nitsch, *Nonlocal damage accumulation and fluid flow in diatomites*, Comm. App. Math. and Comp. Sci, **1** (2006), 143–168.

[6] G. I. Barenblatt, T. W. Patzek, V. M. Prostokishin and D. B. Silin, *SPE75230: Oil deposit in diatomites: A new challenge for subterranean mechanics*, SPE/DOE Improved Oil Recovery Symposium, 2002.

[7] D. Bothe and F. Hilhorst, *A reaction-diffusion system with fast reversible reaction*, J. Math. Anal. Appl., **286** (2003), 125–135.

[8] N. Bouillard, R. Eymard, R. Herbin and P. Montarnal, *Diffusion with dissolution and precipitation in a porous medium: Mathematical analysis and numerical approximation of a simplified model*, ESAIM: M2AN, **41** (2007), 975–1000.

[9] N. Bouillard, R. Eymard, M. Henry, R. Herbin and D. Hilhorst, *A fast precipitation and dissolution reaction for a reaction-diffusion system arising in a porous medium*, Nonlinear Analysis: Real World Applications, **10** (2009), 629–638.

[10] L. M. Cathles, "EQAlt–Equilibrium Chemical Alteration. Combined Physical and Chemical Geofluids Modeling," University of Windsor, Windsor, Ontario, 2006.

[11] J. Chadam, A. Peirce and P. Ortoleva, *Stability of reactive flows in porous media: Coupled porosity and viscosity changes*, SIAM J. Appl. Math., **51** (1991), 684–692.

[12] M. A. J. Chaplain and G. Lolas, *Mathematical modelling of cancer invasion of tissue: Dynamic heterogeneity*, Networks and Heterogeneous Media, **1** (2006), 399–439.

[13] C.-S. Chou, Y.-T. Zhang, R. Zhao and Q. Nie, *Numerical methods for stiff reaction-diffusion systems*, Disc. Cont. Dyn. Syst. - Series B, **7** (2007), 515–525.

[14] A. Dawes, G. Ermentrout, E. N. Cytrynbaum and L. Edelstein-Keshet, *Action filament branching and protrusion velocity in a simple 1D model of a motile cell*, J. Theoretical Biology, **242** (2006), 265–279.

[15] S. Descombes, *Convergence of a splitting method of high order for reaction-diffusion systems*, Math. Comp., **70** (2001), 1481–1501.

[16] S. Descombes and M. Massot, *Operator splitting for nonlinear reaction-diffusion systems with an entropic structure: Singular perturbation and order reduction*, Numer. Math., **97** (2004), 667–698.

[17] C. J. van Duijn and P. Knabner, *Travelling waves in the transport of reactive solutes through porous media: Adsorption and binary ion exchange–Part 1*, Transport Porous Med, **8** (1992), 167–194.

[18] C. J. van Duijn and P. Knabner, *Travelling waves in the transport of reactive solutes through porous media: Adsorption and binary ion exchange–Part 2*, Transport Porous Med, **8** (1992), 199–225.
[19] C. J. van Duijn, P. Knabner and R. J. Schotting, *An analysis of crystal dissolution fronts in flows through porous media. Part 2: Incompatible boundary conditions*, Adv. Water Res., **22** (1998), 1–16.
[20] B. Faugeras, J. Pousin and F. Fontvieille, *An efficient numerical scheme for precise time integration of a diffusion-dissolution/precipitation chemical system*, Math. Comp., **75** (2005), 209–222.
[21] T. Heggheim, M. V. Madland, R. Risnes and T. Austad, *A chemical induced enhanced weakening of chalk by seawater*, J. Pet. Sci. Eng., **46** (2005), 171–184.
[22] F. Hilhorst, R. van der Hout and L. A. Peletier, *The fast reaction limit for a reaction-diffusion system*, J. Math. Anal. Appl., **199** (1996), 349–373.
[23] F. Hilhorst, R. van der Hout and L. A. Peletier, *Nonlinear diffusion in the presence of fast reaction*, Nonlinear Analysis, **41** (2000), 803–823.
[24] F. Hilhorst, J. R. King and M. Roger, *Travelling-wave analysis of a model describing tissue degradation by bacteria*, Euro. J. Appl. Math., **18** (2007), 583–605.
[25] F. Hilhorst, J. R. King and M. Roger, *Mathematical analysis of a model describing the invasion of bacteria in burn wounds*, Nonlinear Analysis, **66** (2007), 1118–1140.
[26] A. Hiorth, L. M. Cathles, J. Kolnes, O. Vikane, A. Lohne and M. V. Madland, *A chemical model for the seawater-CO_2-carbonate system – aqueous and surface chemistry*, Paper prepared for presentation at the Wettability Conference held in Abu Dhabi, UAE, 27–28 october, 2008.
[27] H. Holden, K. H. Karlsen, K.-A. Lie and N. H. Risebro, "Operator Splitting for Nonlinear Partial Differential Equations with Rough Coefficients," book to appear.
[28] P. Knabner, C. J. van Duijn and S. Hengst, *An analysis of crystal dissolution fronts in flows through porous media. Part 1: Compatible boundary conditions*, Adv. Water Res., **18** (1995), 171–185.
[29] R. I. Korsnes, M. V. Madland, T. Austad, S. Haver and G. Rœsland, *The effects of temperature on the water weakening of chalk by seawater*, J. Pet. Sci. Eng., **60** (2008), 183–193.
[30] A. C. Lasaga, "Kinetic Theory in the Earth Sciences," Princeton series in geochemistry, Princeton University Press, 1998.
[31] R. J. LeVeque, "Finite Volume Methods for Hyperbolic Problems," Cambridge Texts in Applied Mathematics, Berlin, 2002.
[32] M. V. Madland, A. Finsnes, A. Alkafadgi, R. Risnes and T. Austad, *The influence of CO2 gas and carbonate water on the mechanical stability of chalk*, J. Pet. Sci. Eng., **51** (2006), 149–168.
[33] M. V. Madland, *Rock-Fluid interactions in chalk exposed to seawater, $MgCl_2$, and NaCl brines with equal ionic strength*, 15th European Symposium on Improved Oil Recovery - Paris, France, 27–29, April 2009.
[34] B. P. Marchant, J. Norbury and A. J. Perumpanani, *Traveling shock waves arising in a model of malignant invasion*, SIAM J. Appl. Math., **60** (2000), 463–476.
[35] B. P. Marchant, J. Norbury and J. A. Sherrat, *Travelling wave solutions to a haptotaxis-dominated model of malignant invasion*, Nonlinearity, **14** (2001), 1653–1671.
[36] E. Maisse and J. Pousin, *Diffusion and dissolution/precipitation in an open porous reactive medium*, J. Comp. Appl. Math., **82** (1997), 279–290.
[37] R. Natalini, C. Nitsch, G. Pontrell and S. Sbaraglia, *A numerical study of a nonlocal model of damage propagation under chemical aggression*, Euro. J. Appl. Math., **14** (2003), 447–464.
[38] Q. Nie, Y.-T. Zhang and R. Zhao, *Efficient semi-implicit schemes for stiff systems*, J. Comput. Physics, **214** (2006), 521–537.
[39] D. A. Nield and A. Bejan, "Convection in Porous Media," Springer Verlag, 1992.
[40] C. Nitsch, *A nonlinear parabolic system arising in damage mechanics under chemical aggression*, Nonlinear Analysis, **61** (2005), 695–713.
[41] A. Pawell and K.-D. Krannich, *Dissolution effects in transport in porous media*, SIAM J. Appl. Math., **56** (1996), 89–118.
[42] J. Pousin, *Infinitely fast kinetics for dissolution and diffusion in open reactive systems*, Nonlinear Analysis, **39** (2000), 261–279.

[43] K. Promislow, J. Stockie and B. Wetton, *Sharp interface reduction for multiphase transport in a porous fuel cell electrode*, Proceedings of the Royal Society of London, Series A, **462** (2006), 789–816.
[44] T. Roose, S. J. Chapman and P. K. Maini, *Mathematical models of avascular tumor growth*, SIAM Review, **49** (2007), 179–208.
[45] M. Schatzmann, *Toward non commutative numerical analysis: high order integration in time*, J. Sci. Computing, **17** (2002), 107–125.
[46] J. A. Sherrat and M. A. J. Chaplain, *A new mathematical model for avascular tumor growth*, J. Math. Biol., **43** (2001), 291–312.
[47] C. I. Steefel and A. C. Lasaga, *A coupled model for transport of multiple chemical species and kinetic precipitation/dissolution reactions with application to reactive flow in single phase hydrothermal systems*, American J Sci., **294** (1994), 529–592.
[48] G. Strang, *On the construction and comparison of difference schemes*, SIAM J. Num. Anal., **5** (1968), 506–517.
[49] L. Yu, S. Evje, I. Fjelde, H. Kleppe, T. Kaarstad and S. M. Skjaeveland, *Modelling of wettability alteration processes in carbonate oil reservoirs*, Networks and Heterogeneous Media, **3** (2008), 149–183.

Received April 2009; revised August 2009.

E-mail address: steinar.evje@iris.no
E-mail address: aksel.hiorth@iris.no
E-mail address: merete.v.madland@uis.no
E-mail address: reidar.i.korsnes@uis.no